İSTANBUL UNIVERSITY-CERRAHPAŞA
INSTITUTE OF GRADUATE STUDIES

M.Sc. THESIS

INVESTIGATION OF METAL ION RELEASE FROM BIOMEDICAL IMPLANT MATERIALS

Helal HASSOUN

SUPERVISOR
Prof. Dr. İlven MUTLU

Nanoscience and Nanoengineering

Nanoscience and Nanoengineering

August, 2022

THESIS ACCEPTANCE AND APPROVAL

This thesis titled " Investigation of Metal Ion Release from Biomedical Implant Materials", prepared by **Helal HASSOUN** under the supervision of **Prof. Dr. İlven MUTLU**, was accepted as a **M.Sc. Thesis** after being **consensus** approved by our jury as a result of the exam held on **26/08/2022**.

Examining Committee Members

		Signature	Decision
SUPERVISOR	Prof. Dr. İlven MUTLU Istanbul University-Cerrahpasa Metallurgical and Materials Engineering Department		☒ Accept ☐ Reject
MEMBER	Prof. Dr. ---- İstanbul University-Cerrahpasa ----------		☒ Accept ☐ Reject
MEMBER	Prof. Dr. ------ ------ -------		☒ Accept ☐ Reject

DECLARATION

I hereby declare that this thesis is my own work, I have not had engaged in any unethical behavior at any of the stages from planning to the writing of the thesis, I have obtained all the information in this thesis within the limits of the academic and scientific ethical rules, I have cited all the information and comments being obtained in this thesis study, and I have included these references in the list of references. During the analysis and writing stages of this thesis, I accept that I have abided by the patent and copyright rights and therefore I myself take all kinds of legal responsibility.

Helal HASSOUN

(Signature)

To My My Family… …

FUNDING

THESIS TITLE

This thesis was supported by the project number 36358 of the İstanbul University-Cerrahpaşa Scientific Research Projects Executive Secretariat.

ACKNOWLEDGEMENT

I wish to expres my special thanks to my family

August, 2022 Helal HASSOUN

CONTENTS

Page

LIST OF FIGURES

Page

LIST OF TABLES

Page

LIST OF SYMBOLS AND ABBREVIATIONS

Symbols	Description
Cu	: Copper
Fe	: Iron
Mg	: Magnesium
Zn	: Zinc

Abbreviations	Description
GPa	: Giga Pascal
MPa	: Mega Pascal
OCP	: Open circuit potential
SEM	: Scanning electron microscope

GENİŞLETİLMİŞ ÖZET

YÜKSEK LİSANS TEZİ

BİYOMEDİKAL İMPLANT MALZEMELERİNDEN METAL İYON SALINIMININ ARAŞTIRILMASI

Helal HASSOUN

İstanbul Üniversitesi-Cerrahpaşa

Lisansüstü Eğitim Enstitüsü

Nanobilim ve Nanomühendislik Anabilim Dalı (İng.)

Nanobilim ve Nanomühendislik Programı

Danışman : Prof. Dr. İlven MUTLU

Bu çalışmada, sert doku onarımı için geçici biyomedikal implant amaçlı biyobozunur metalik (Fe, Zn, ve Mg) alaşımlar üretilmiş ve incelenmiştir. Biyobozunur metalik alaşımlar (Fe, Zn, ve Mg) mekanik alaşımlama-toz metalurjisi yöntemi ile üretilmiştir. Sert doku amaçlı geçici biyomedikal implantlar, gerilim gevşemesini önlemek için kemiğe yakın elastisite modülüne, kemik iyileşme hızına yakın optimum bir biyobozunma hızına ve yeterli biyouyumluluk seviyesine sahip olmalıdır. Öncelikle, metal tozları bilyeli değirmende işlem görmüş (mekanik alaşımlama), ardından polimer esaslı bağlayıcı ilave edilmiş, ardından karışım preslenerek ham numuneler üretilmiş ve son olarak ham numuneler sinterlenmiştir. Alaşımların elektrokimyasal korozyon özellikleri yapay vücut sıvısında potansiyostat yardımı ile incelenmiştir. Ayrıca alaşımların metal iyon salınımı (Fe, Zn, ve Mg) ve ağırlık değişimi özellikleri yapay vücut sıvısı içerisinde incelenmiştir.

Ağustos 2022 , 72. sayfa.

Anahtar kelimeler: Biyomalzeme, ortopedik implant, toz metalurjisi, biyobozunur metal

ABSTRACT

M.Sc. THESIS

INVESTIGATION OF METAL ION RELEASE FROM BIOMEDICAL IMPLANT MATERIALS

Helal HASSOUN

İstanbul University-Cerrahpaşa

Institute of Graduate Studies

Department of Nanoscience and Nanoengineering

Nanoscience and Nanoengineering Programme

Supervisor : Prof. Dr. Ilven MUTLU

In this study, biodegradable metal (Fe, Zn, and Mg) alloys for temporary biomedical implant for hard tissue repair applications were fabricated and investigated. Biodegradable metal alloys (Fe, Zn, and Mg) were fabricated by mechanical alloying-powder metallurgy method. Temporary biomedical implants for hard tissue applications, must show elastic modulus close to bone (to prevent stress-shielding effect), must show optimum biodegradation rate close to bone healing rate, and must have suitable biocompatibility level. Initially, metal powders were processed in ball mill (mechanical alloying), then polymer based binder was included, then the mixture was compacted and green specimens were fabricated, and lastly the green specimens were sintered. Electrochemical corrosion properties of the alloys were investigated in simulated body fluid with potentiostat. In addition, metal ion (Fe, Zn, and Mg) release and weight change properties of the alloys were investigated in simulated body fluid.

August 2022, 72. pages.

Keywords: Biomaterial, orthopaedic implant, powder metallurgy, Biodegradable metal

1. INTRODUCTION

In the present study, biodegradable metal (Fe, Zn, and Mg) alloys for temporary biomedical implant applications were fabricated and investigated. Biodegradable metal alloys (Fe, Zn, and Mg) were fabricated by mechanical alloying-powder metallurgy method. Temporary biomedical implants for hard tissue applications, must show elastic modulus close to bone (to prevent stress-shielding effect), must show optimum biodegradation rate close to bone healing rate, and must have suitable biocompatibility level. Initially, metal powders were processed in ball mill (mechanical alloying), then polymer based binder was included, then the mixture was compacted and green specimens were fabricated, and lastly the green specimens were sintered. Electrochemical corrosion properties of the alloys were investigated in simulated body fluid with potentiostat. In addition, metal ion (Fe, Zn, and Mg) release and weight change properties of the alloys were investigated in simulated body fluid.

In general, biomaterial is a systemically and pharmacologically inert material manufactured for implantation within or incorporation with living systems. In general, biomaterials are a group of advanced engineering materials. In the periodic table, although approximately 75 % of the elements are metals, small number metals can be employed in the biomedical applications due to their low biocompatibility caused by electrochemical corrosion. European Society for Biomaterials descibed the biomaterial as a “non-viable material used in a medical device, intended to interact with biological systems.” The definition was revised as “material intended to interface with biological systems to evaluate, treat, augment or replace any tissue, organ or function of the body.” In general, the biomaterials are sysnthetic materials employed for their mechanical properties, not biological properties. In general, biocompatibility can be defined as “the ability of a material to perform with an appropriate host response in a specific application”. Another definition of the biocompatibility is “the condition of being compatible with living tissue by virtue of a lack of toxicity or ability to cause immunological rejection” [9]. In general, biomedical implant can be described as a medical device, which is manufactured by biomaterials, used in the living body. The biomedicsl implants are employed in the lining body in order to replace or repair of damaged tissue/organs [1-12].

2. CONCEPTUAL FRAMEWORK

2.1. BIODEGRADABLE METALS

In general, biomaterial is a systemically and pharmacologically inert material manufactured for implantation within or incorporation with living systems. Biomaterials are a group of advanced engineering materials. In the periodic table, although approximately 3/4 of the elements are metal, small number metals can be employed in the biomedical applications due to their low biocompatibility (materials with low toxicity) which is attributed to their electrochemical corrosion.

The term “biomaterial (biocompatible materials)” can be desribed as nonliving material group employed in a biomedical device, aimed to interact with biological organs/tissues. This definition, also can be changed as material group aimed to interface with biological tissue/organs in order to repair, treat, heal or replace any living organ or tissue.

In general, the biomaterials (biocompatible materials) are sysnthetic materials employed in the body mainly for their mechanical properties, but not biological properties.

In general, biocompatibility can be defined as the behaviour of a material, which shows a suitable host response in a definite application [9].

In general, biomedical implants can be described as a medical device, which is manufactured by biomaterials, used in the living body. The biomedicsl implants are employed in the lining body in order to replace or repair of damaged tissue/organs [1-12].

The critical parameters of a surface are the chemistry (nature of chemical groups and their reactions with surrounding tissue), topography (roughness or design), and the physical properties (porosity, stiffness). Protein absorption and cell adhesion are main properties of the biomedical implant materials. Surface chemistry, surface topography, surface mechanical properties, cell proliferation (cell grows and divides), cell differentation (dividing cells change their type), ECM (extracellular matrix) produciction, apoptosis (programmed celll death) are important properties in the biomedical implants. Figure 2.1 illustrates the interaction between an biomedical implant surface and the biological systems.

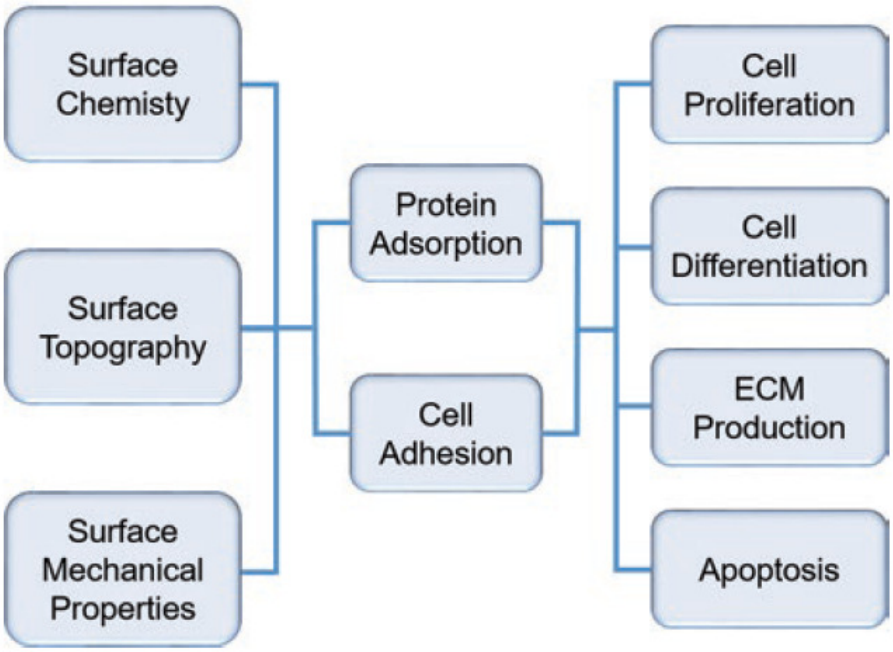

Figure 2.1. Interaction between implant surface and biological system [9]

Figure given below, clearly illustates the time frame (in days) of the inflammation process and cell involvement [9]. Coagulation (shortest stage), inflammation, migration/proliferation (longest stage), and remodelling (last stage) are the main parts of the process. Formation of the platelets, neutrophils, macrophages, fibroblats and lymphocytes can be seen.

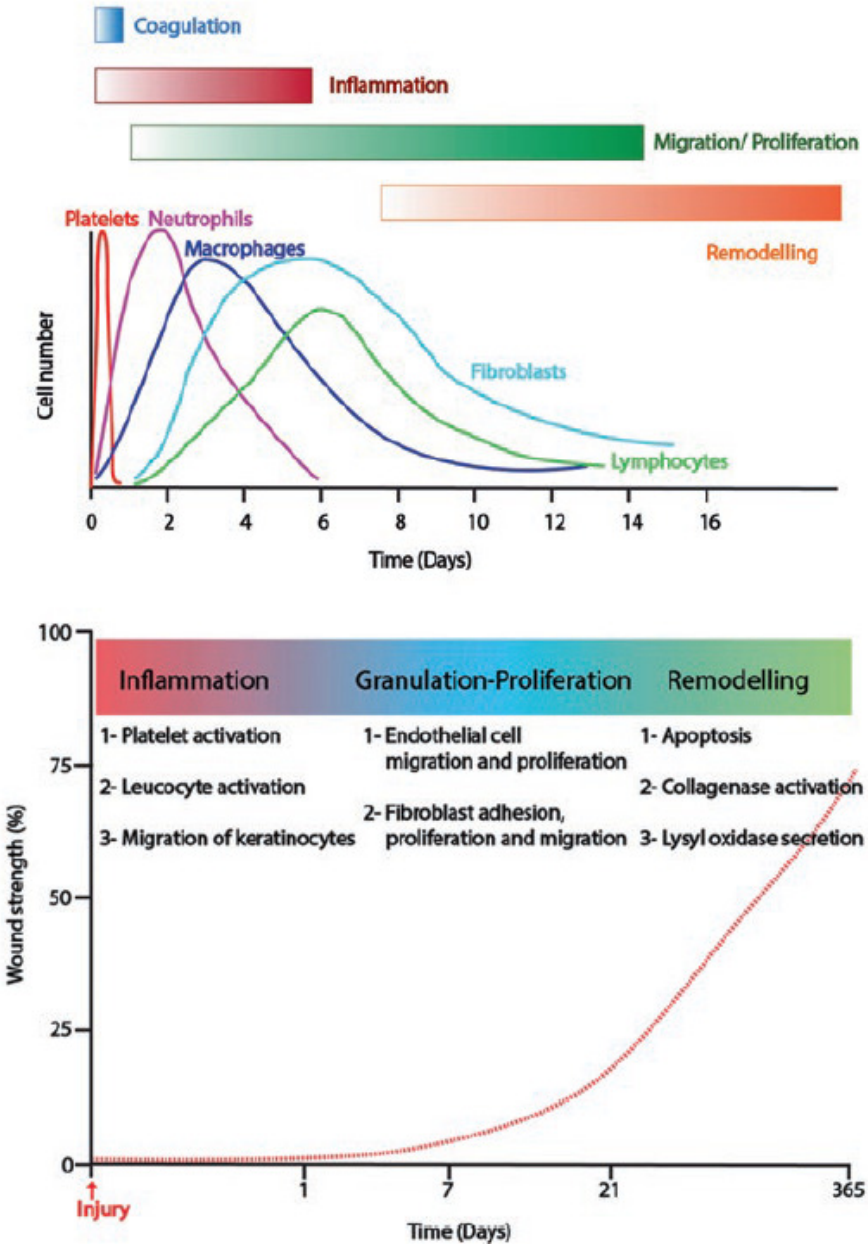

Figure 2.2. Time frame of inflammation and cell involvement [9]

Cell proliferation (growth and division at same time) can be defined as growing and dividing of cells in order to produce 2 cells. Cell proliferation increase the total number of cells and produce tissue growth. In general, inflammation can be defined as complicated response (biological) of living body/tissue to stimulations (irritation, pathogen, damaging cells) and protective response (blood vessels, immune cells). Regeneration can be defined as restoration process and tissue growing process.

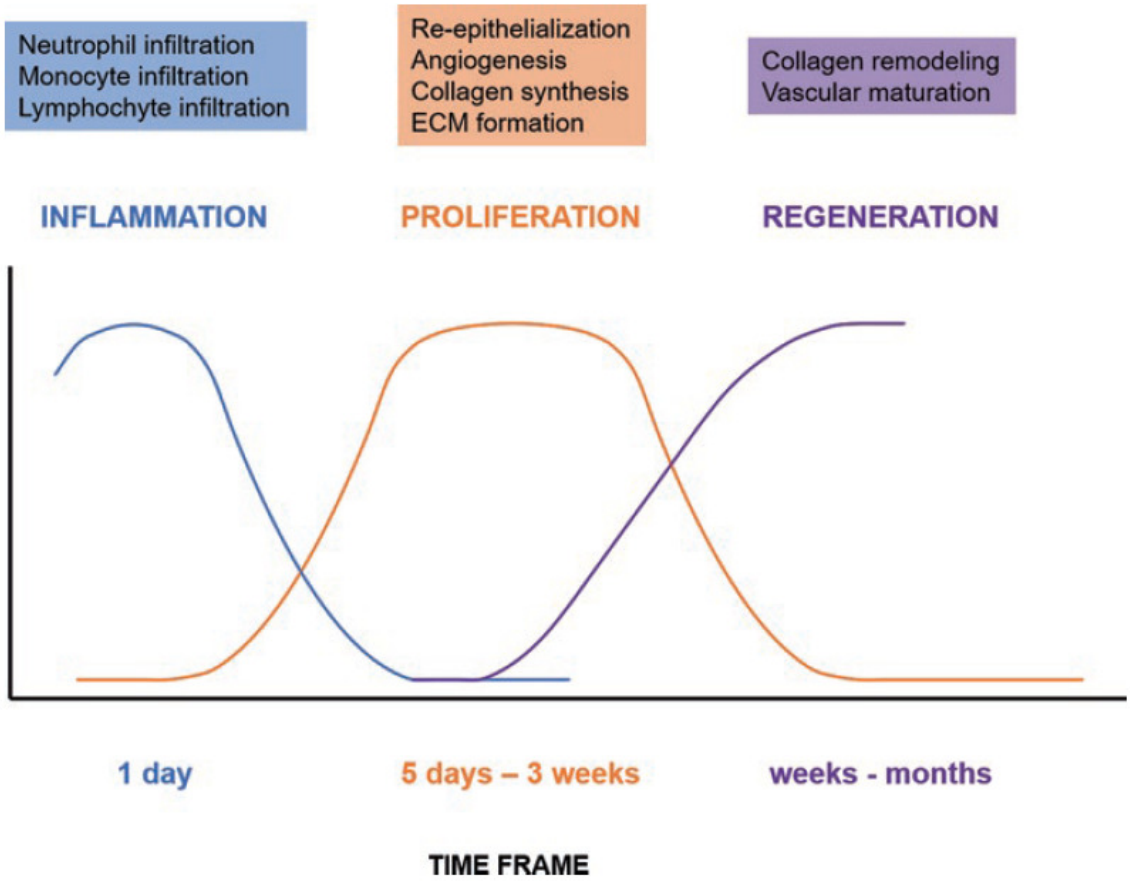

Figure 2.3. Repair process [9]

In general, desription of the biodegradable metal is “group of metals, which are expected to show corrosion gradually in vivo, with suitable tissue/organ response produced by the electrochemical corrosion (biodegradation) products, which can be metabolized or absorbed by the living cells, and then dissolve fully to assist with proper tissue healing without implant residues.” Figure given below schematicaly illustrates the bone fracture repair (osteoblasts, osteoclasts, bone trabecula etc). Also, chemical reactions and products can be seen in the figüre.

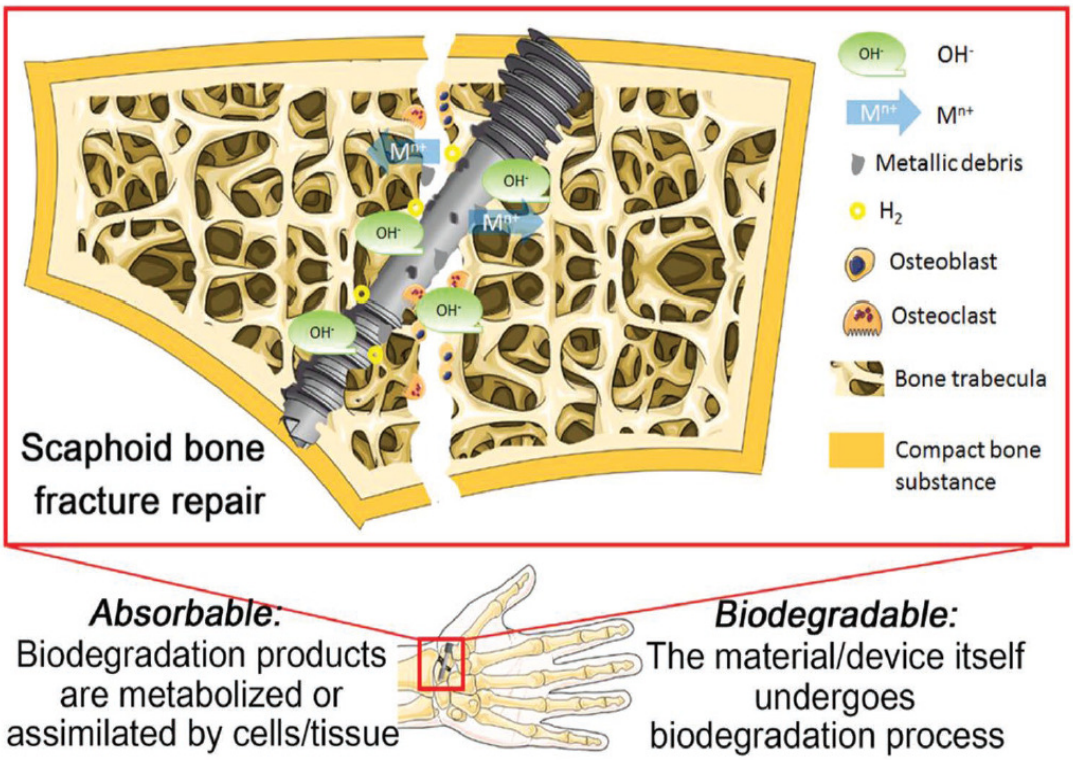

Figure 2.4: Usage of bioabsorbable or biodegradable terms [11]

Figure given below, schematicaly illustrates the important parameters for the biodegradable (bioabsorbable) metals. In general, the biodegradable metals must be biodegradable and biocompatible (to cells, tissue, and humans). In the design of the biodegradable metals, mechanical properties, physical properties, chemical properties, and biological properties must be consider.

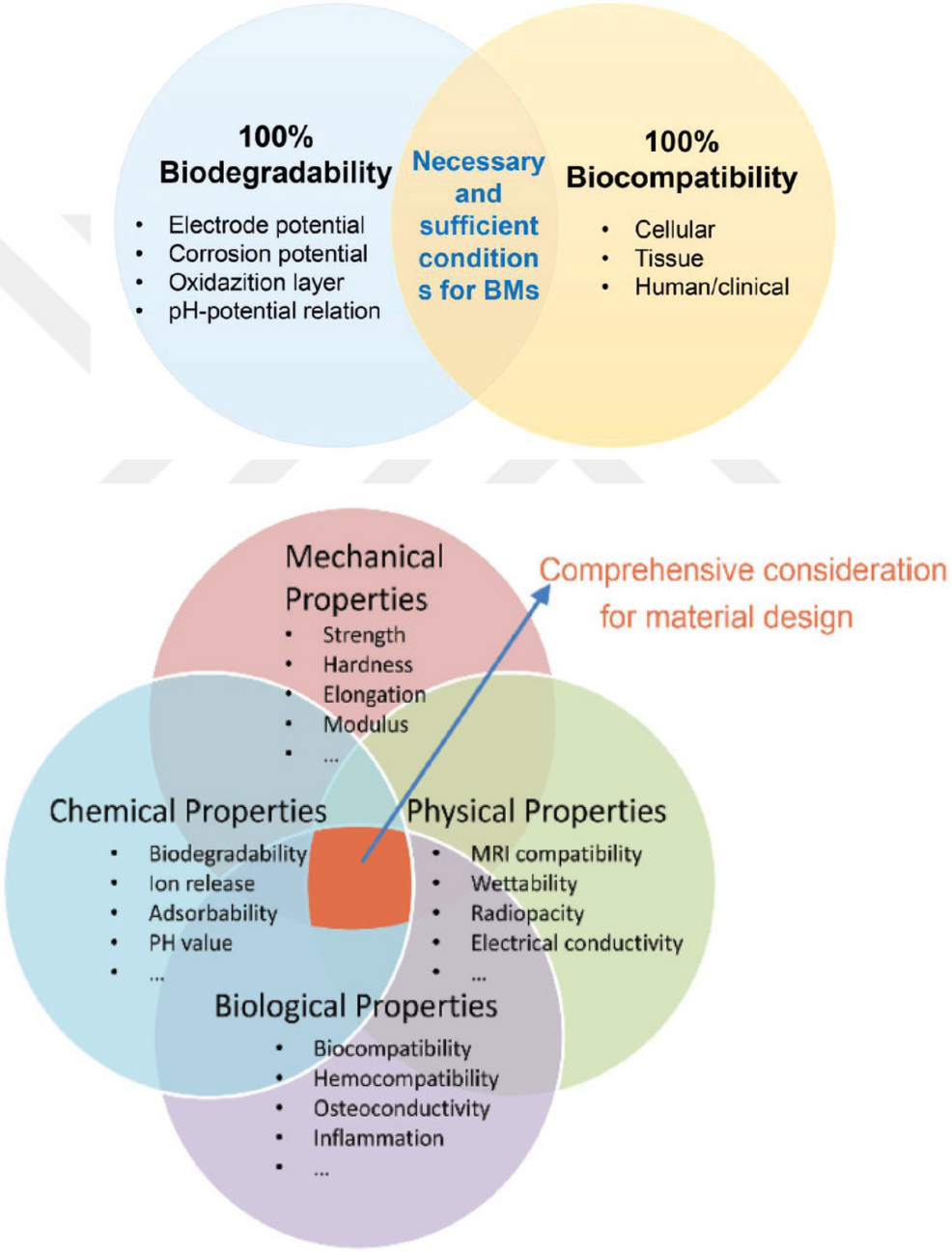

Figure 2.5. Important parameters for biodegradable metals [11]

Figure given below shows the standard electrode potential values, which reflects the biodegradation rate (hydrogen evolution or/and oxygen absorption), of the metallic elements. As seen from the figüre, in some elements biodegradation is by hydrogen evolution and oxygen absorption. In some elements biodegradation is only by oxygen absorption.

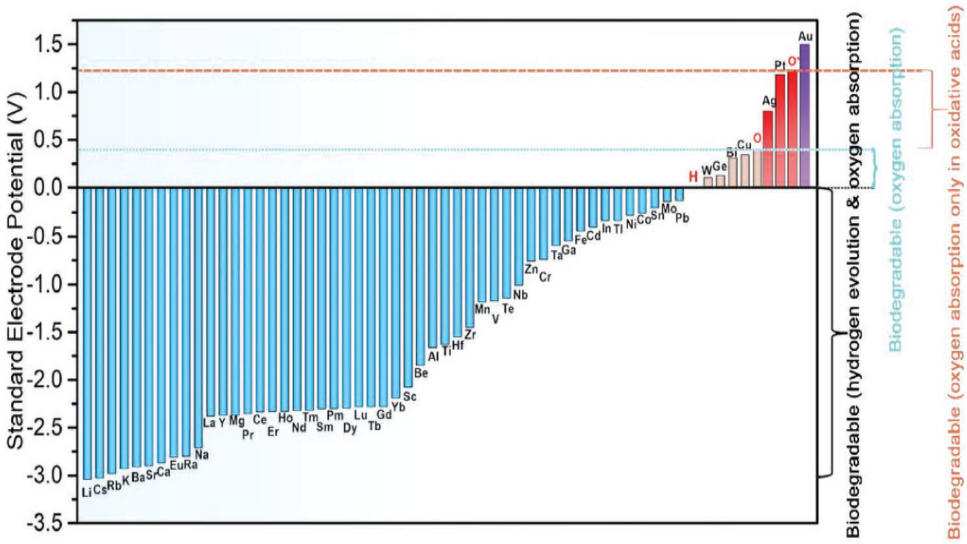

Figure 2.6. Standard electrode potential-biodegradation relationship of metallic elements

Figure given below, illustrates the reactivity serie values of the pure metals in important aqueous environments (water, strongoxidizing acids, steam, mineral acids, boiling water, cold water).

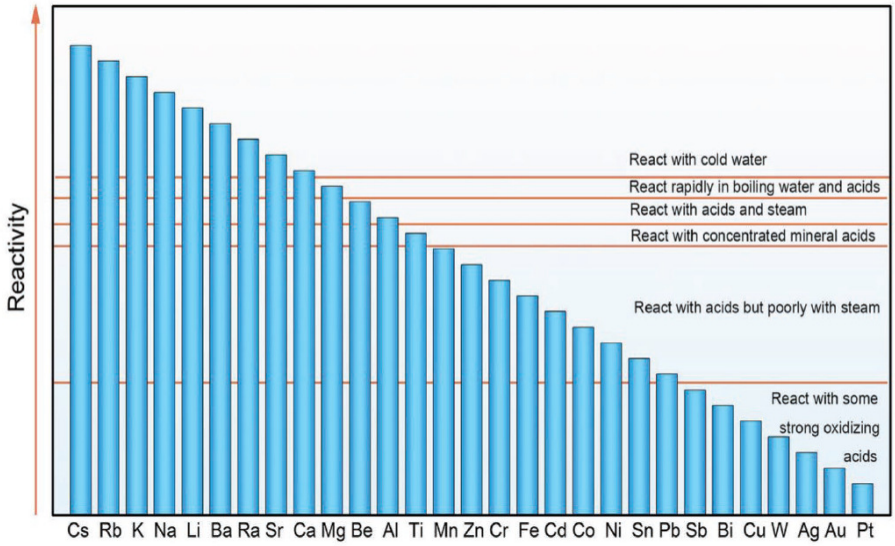

Figure 2.7. Reactivity series of pure metals in various aqueous environments

Figure given below, illustrates the Pilling-Bedworth Ratio (R_{PB}) and standard electrode potential (V) values of the several metals. In general, there are three possibility according to the Pilling-Bedworth ratio (R_{PB})

- Leakage or cracking on the oxide film formation can be seen in the metals having Pilling-Bedworth ratio (R_{PB}) higher than 2.0.
- Compressive-strengthened, compact oxide film formation can be seen in the metals having Pilling-Bedworth ratio (R_{PB}) between 1.0-2.0.
- Loose and thin oxide film formation can be seen in the metals having Pilling-Bedworth ratio (R_{PB}) lower than 1.0.

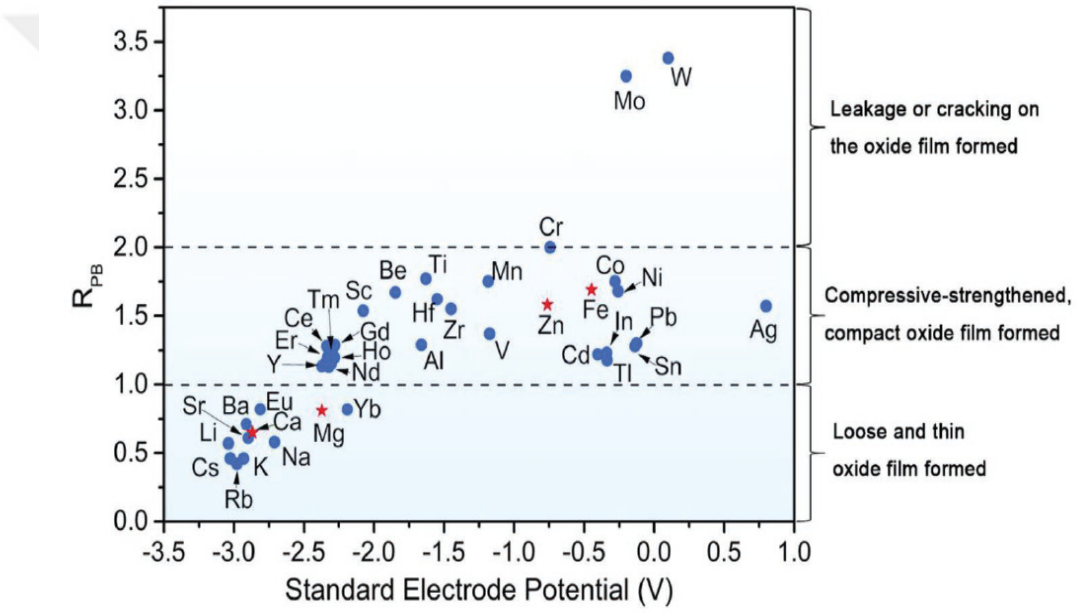

Figure 2.8. Pilling-Bedworth ratio and standard electrode potentials of metals [11]

Figure given below, shows the general classification of the metallic elements in the living human body conditions.

- Major elements are: Ca, K, Na, and Mg.
- Trace elements are: Cr, Fe, Cu, Mn, Co, Mo, V, Ni, Zn, Li
- Nonesential but usefull elements are: Sn, Sr, Ge
- Nontoxic trace elements with unknown functions: Al, Bi, Ba, Au, Ag, Zr, W, RE

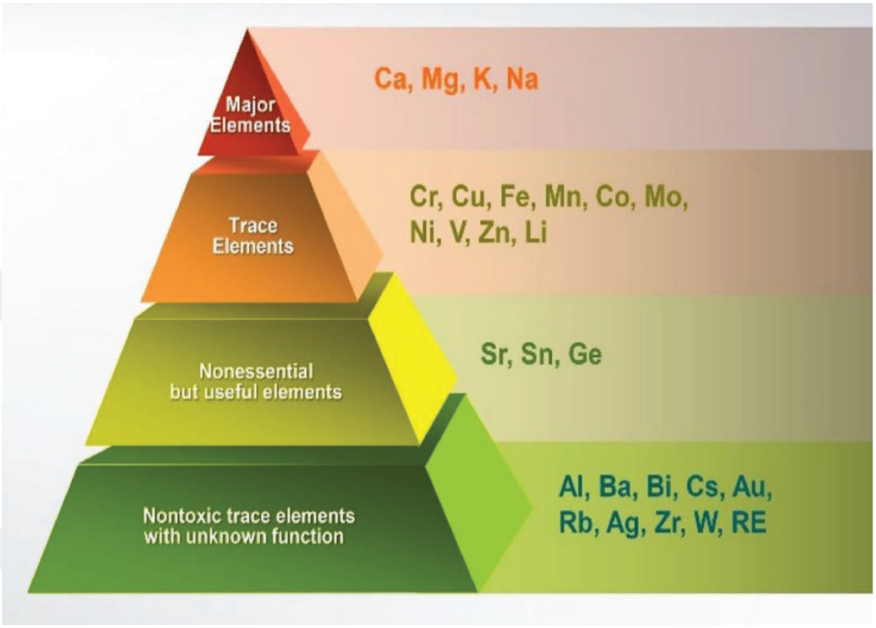

Figure 2.9. Classification of metallic elements in the living human body [11]

Figure given below, schematicaly illustrates the general mechanism (reaction steps) of the biocorrosion at the biomedical implant-body fluid interface.

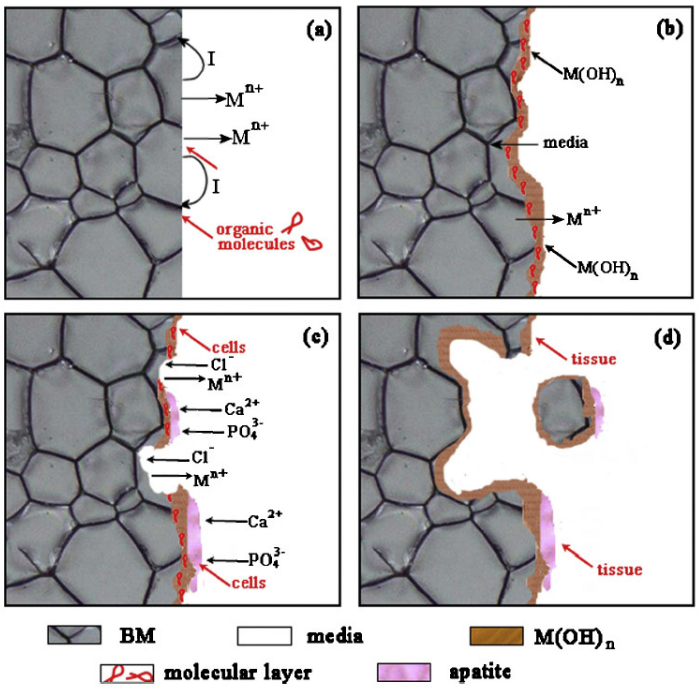

Figure 2.10: Biocorrosion mechanism at implant-body fluid interface [17]

Figure given below, illustrates the biodegradation process and the mechanical properties of the biomedical implant materials during the inflammation (7 days), repair (3-6 months) and remodelling (years) stages.

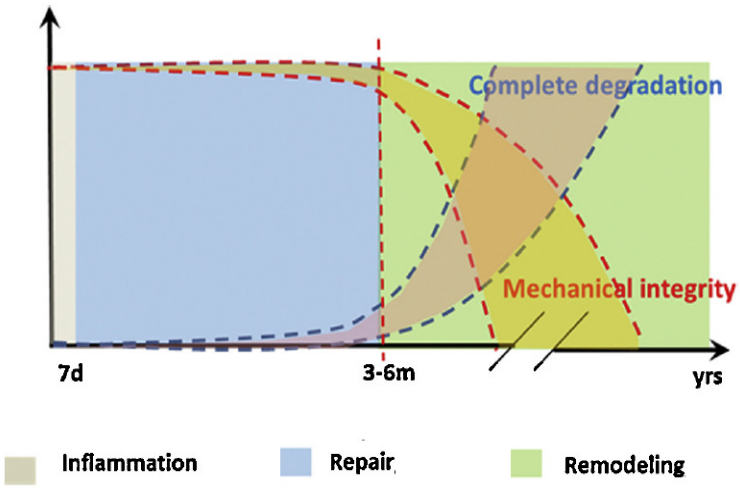

Figure 2.11: **Biodegradation and mechanical properties of implant materials [17]**

2.2. ELECTROCHEMICAL CORROSION

Corrosion can be desribed as “attack on a material (usually metal) by electrochemical reaction with its environment. There are (i) wet corrosion (environment is water), (ii) dry gas (chemical) corrosion (at high temperatures) and (iii) corrosion in the salts/melt metals. There are several types of corrosion such as: uniform (general) corrosion, galvanic (two-metal) corrosion, crevice corrosion, pitting corrosion, intergranular corrosion (exfoliation), hydrogen damage, dealloying, cavitation, erosion, fretting, stress corrosion.

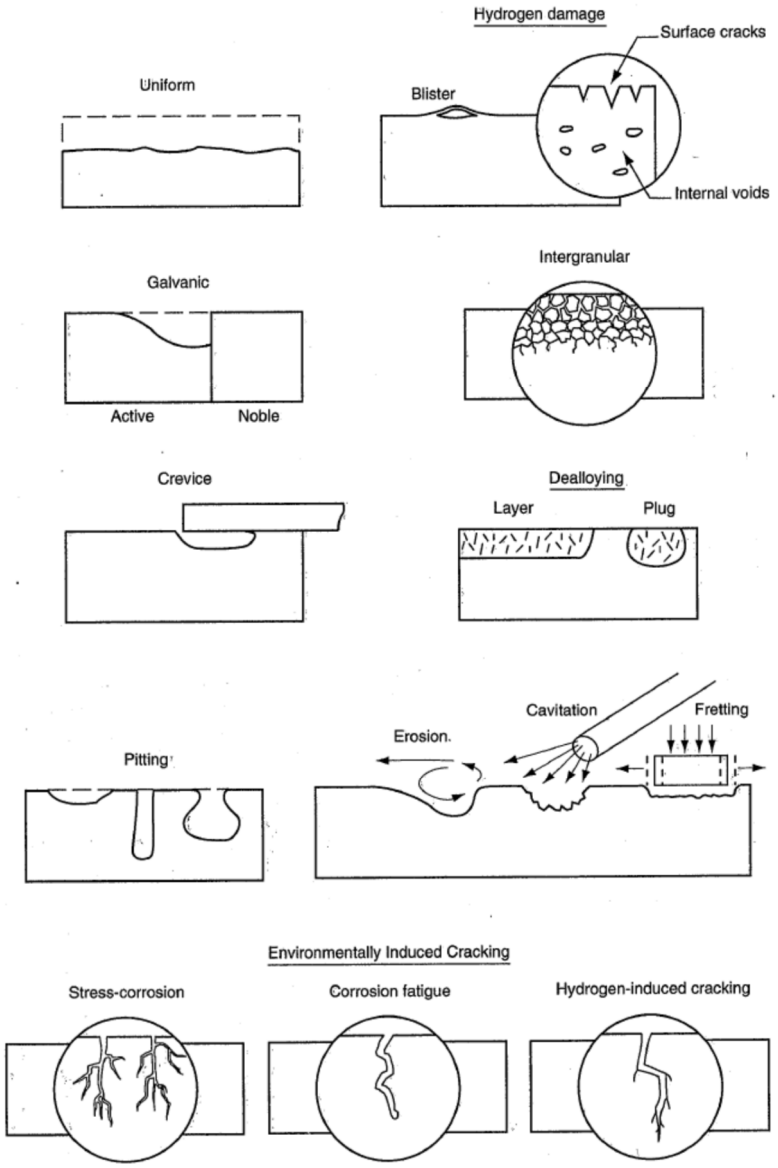

Figure 2.12: Types of corrosion [14]

Fort he electrochemical corrosion to take place, a electrochemical corrosion cell must be formed. A electrochemical corrosion cell consits of the following 4 parts: anode, cathode, electrolyte (ionic conduction), and metallic path (electrical conduction).

Table given below, illustrates the standard electromotive force values of several metals. As seen from the table, potassium (K) and sodium (Na are the most active metals, while gold (Au) is the most noble metal. Iron (Fe) is in the relatively upper side of the table. Zinc (Zn) is at the relatively lower side, while magnesium (Mg) is at the bottom of the table.

Table 2.1: Standars electromotive force potentials (reduction) [14]

	Reaction	Standard Potential, e° (volts vs. SHE)
Noble	$Au^{3+} + 3e^- = Au$	+1.498
	$Cl_2 + 2e^- = 2Cl^-$	+1.358
	$O_2 + 4H^+ + 4e^- = 2H_2O$ (pH 0)	+1.229
	$Pt^{2+} + 3e^- = Pt$	+1.118
	$NO_3^- + 4H^+ + 3e^- = NO + 2H_2O$	+0.957
	$O_2 + 2H_2O + 4e^- = 4OH^-$ (pH 7)*a*	+0.82
	$Ag^+ + e^- = Ag$	+0.799
	$Hg_2^{2+} + 2e^- = 2Hg$	+0.799
	$Fe^{3+} + e^- = Fe^{2+}$	+0.771
	$O_2 + 2H_2O + 4e^- = 4OH^-$ (pH 14)	+0.401
	$Cu^{2+} + 2e^- = Cu$	+0.342
	$Sn^{4+} + 2e^- = Sn^{2+}$	+0.15
	$2H^+ + 2e^- = H_2$	0.000
	$Pb^{2+} + 2e^- = Pb$	−0.126
	$Sn^{2+} + 2e^- = Sn$	−0.138
	$Ni^{2+} + 2e^- = Ni$	−0.250
	$Co^{2+} + 2e^- = Co$	−0.277
	$Cd^{2+} + 2e^- = Cd$	−0.403
	$2H_2O + 2e^- = H_2 + 2OH^-$ (pH 7)[a]	−0.413
	$Fe^{2+} + 2e^- = Fe$	−0.447
	$Cr^{3+} + 3e^- = Cr$	−0.744
	$Zn^{2+} + 2e^- = Zn$	−0.762
	$2H_2O + 2e^- = H_2 + 2OH^-$ (pH 14)	−0.828
	$Al^{3+} + 3e^- = Al$	−1.662
	$Mg^{2+} + 2e^- = Mg$	−2.372
	$Na^+ + e^- = Na$	−2.71
Active	$K^+ + e^- = K$	−2.931

Table given below, illustrates the galvanic series of several metals in the seawater conditions (dark boxes on the table show the active behaviour). As seen from the table, Mg is the most active metal, while graphite and platinum are the most noble. Fe alloys are in the relatively upper side of the table. Zn alloys are at the relatively lower side, while Mg alloys are at the bottom of the table (very active).

Table 2.2: Galvanic series in seawater (dark boxes show active behaviour) [14]

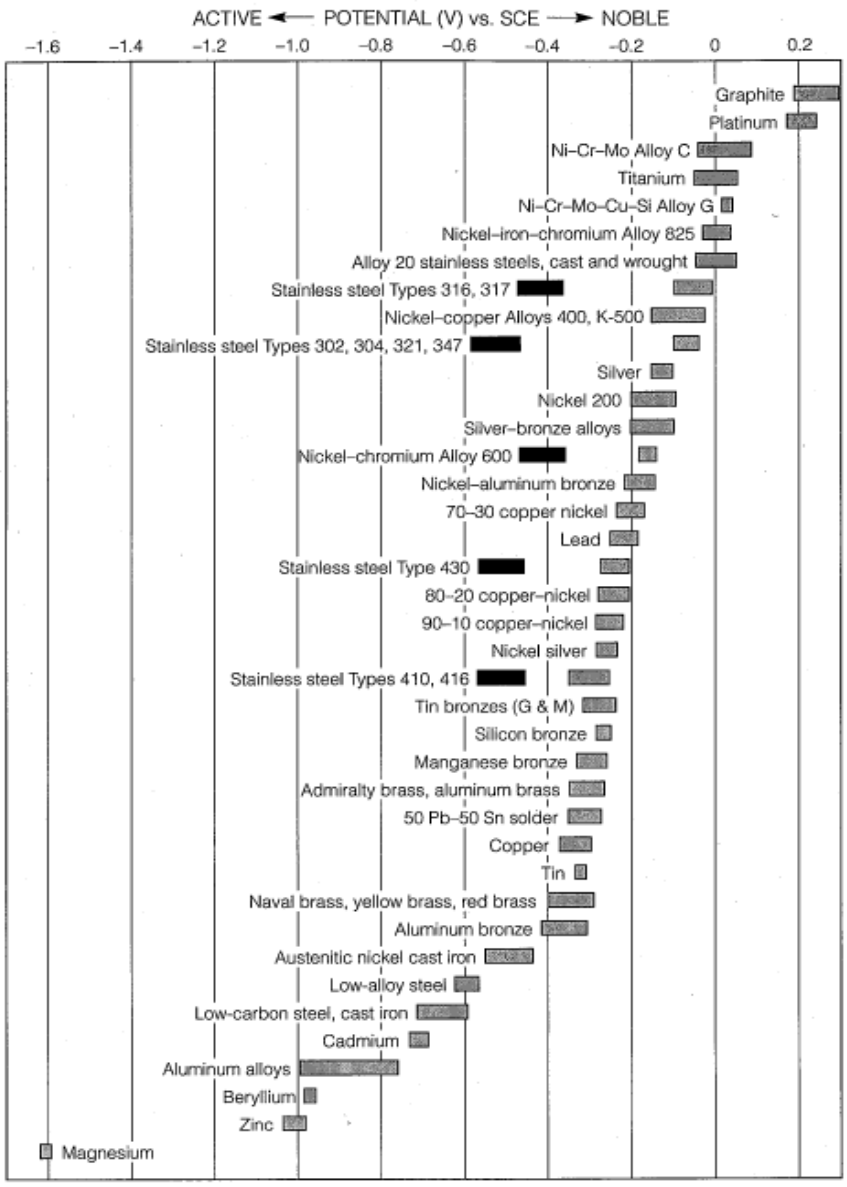

Pourbaix Stability Diagrams (pH-Potential Diagrams)

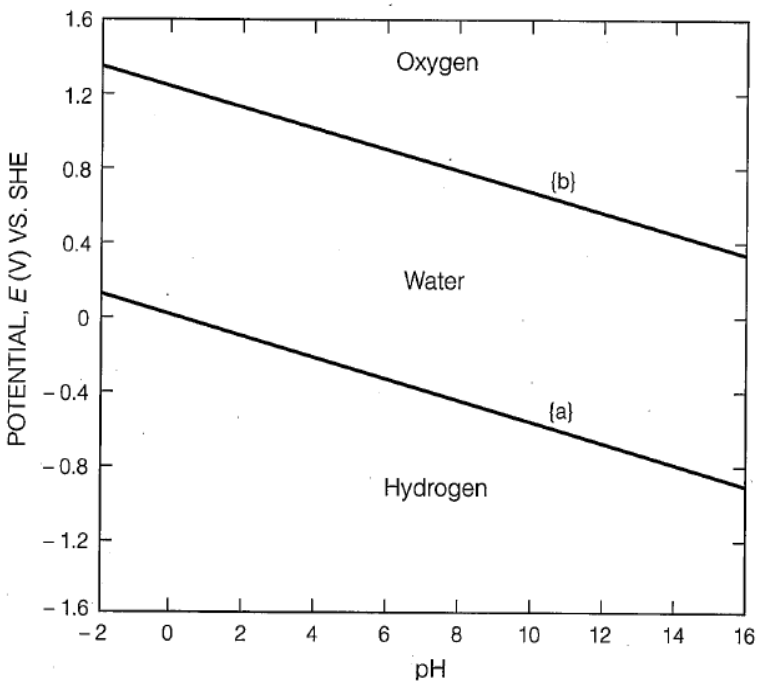

Figure 2.13: Pourbaix diagram for water (stability and decomposition products) [14]

pH is very important parameter in water based solutions, and affects the equilibrium potentials of possible reactions. Pourbaix stability diagrams (pH-potential diagrams) can be used in the determination of the possibilities of the corrosion. The pH-potential diagrams are representation of the Nernsts equation for the several reactions.

The aims of the pH-potential diagrams are;

- illustrates the directions of several reactions at specific potential and pH,
- calculation of the corrosion product compositions at several potential and pH conditions,
- illustrates which potential and pH will decrease or stop the corrosion.

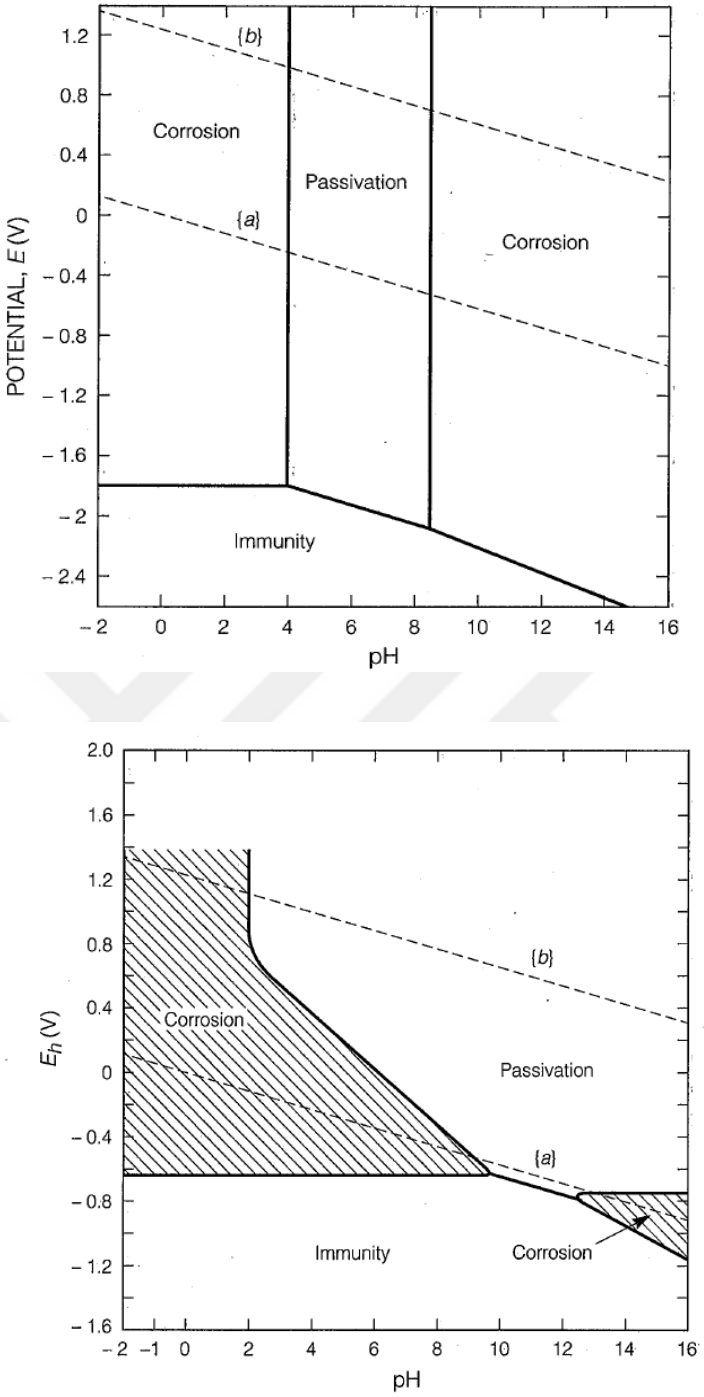

Figure 2.14: Pourbaix diagrams a) aluminium, b) iron [14]

2.3 LITERATURE REVIEW

Yang et al. [4], implanted zinc coronary stent metrials into the rabbits. The Zn alloy based stent was not changed its integrity for up to 24 weeks and degraded 40 % after 52 weeks. There was no any thrombosis, inflammation, or other cases in the rabbits.

Vojtech et al. [6] have prepared Zn-Mg alloys with 3 % Mg. The alloys were exhibited corrosion rates (biodegradation) lower than the Mg.

Zhao et al. [7] have found that, Zn-Li alloy wire, which implanted into the aorta of rats has suitable biocompatibility.

Bowen et al. [15] examined the in vivo corrosion behaviour of the Zn sample and found good biocompatibility in the lumen of rats. They have stated that the corrosion rate is close to the recommended bio-degradation rate for the scaffolds.

Drelich et al. [16] found that Zn wires in the murine artery shows stable corrosion up to a period of 2 years. Zn stents could degrade in 12-24 months. Open-cell (interconnected) porous parts can be manufactured by using the powder metallurgy. There are no solubility limitations in powder metallurgy as compared with casting. Repeatability of the powder metallurgy method is also superior.

Sadighikia et al. [18] have manufactured Zn foams with interconnected open-cellular porous microstructure by using powder metallurgy based space holder (pore former) technique. They used carbamide as a pore former.

Azizi et al. [19] fabricated and studied bulk/nonporous Zn-Al-Cu based alloy by using convent ional powder metallurgy method.

Berent et al [20] studied cast Zn-Al-Si alloy specimens. Alloys based on the eutectic Zn-Al composition are considered, as they show a higher melting temperature, lower corrosion rate, and enhanced mechanical properties. Including of the Si to the Zn-Al based alloys not only

stops the growth of microstructural phases at the interface but also increases the mechanical properties.

Kafri et al. [21] studied metallic Zn-Fe alloy for biodegradable implant applications. Fe was used as a cathodic alloying element in the Zn in order to adjust the biodegradation rate (corrosion rate) by the micro-galvanic effect produced by secondary phases. Zn-Fe alloy specimens were manufactured by casting. Electrochemical corrosion rate of the Zn-Fe alloy specimens was higher than the pure Zn specimens.

3. METHOD

In this study, iron (Fe), magnesium (Mg), and zinc (Zn) alloy specimens were fabricated by using fine Zn powders, Fe powders and magnesium (Mg) powders. Iron (Fe), magnesium (Mg), and zinc (Zn) alloy specimens were manufactured by conventional powder metallurgy-mechanical alloying route, which consisted of powder mixing, mechanical alloying, pressing and sintering stages. Compaction pressure was about 250-300 MPa. Sintering of the Fe alloy specimens was carried out at 1200 °C under vacuum. Sintering of the Zn alloy specimens was carried out at 310 °C under vacuum. Sintering of the Mg alloy specimens was carried out at 510 °C under vacuum. Figure 2.1 shows (a) ball mill (mechanical alloying) and hydraulic press, and (b) sintering furnace and vacuum pump.

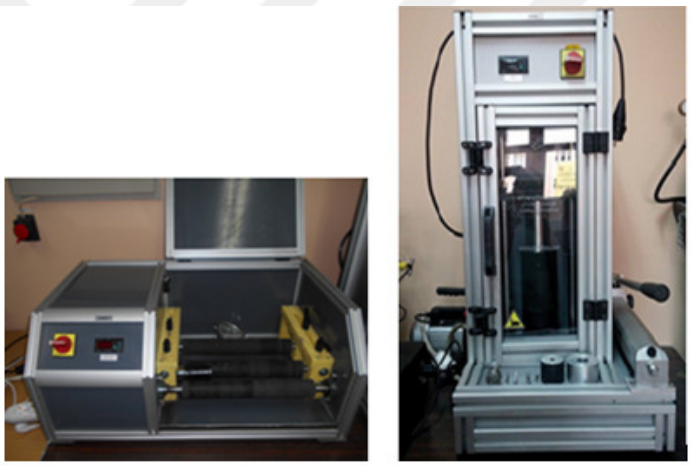

(a)

(b)

Figure 3.1: a) Ball mill and hydraulic press, b) sintering furnace

In this study, zinc alloy specimens were manufactured by using Zn powders, Fe powders and copper (Cu) powders. Zinc alloy specimens were manufactured by conventional powder metallurgy-mechanical alloying method. Wide range of metal alloy compositions can be fabricated by using mechanical alloying. There is no any phase diagram (solid solubility) restrictions in the mechanical alloying (ball milling). Table given below shows the amounts of alloying elements in the Zn alloys.

- Iron (Fe) was included in order to decreaase the biodegradation rate of the Zn. In general biodegradation rate of the pure Zn is higher than bone healing time.
- Iron (Fe) was also included in order to enhance the mechanical properties of the Zn. In general, pure zinc is very brittle metal.
- Copper (Cu) was included in order to enhance the mechanical properties of the Zn. In general, pure zinc is very brittle metal. Cu also provides antibacterial properties to the Zn.

Table 3.1: Amounts of alloying elements in the Zn alloys

Alloy	Zn	Fe	Cu
Zn-5Fe	95	5	
Zn-10Fe	90	10	
Zn-15Fe	55	15	
Zn-5Cu	95		5
Zn-10Cu	90		10
Zn-15Cu	85		15
Zn-15Fe-5Cu	80	15	5
Zn-10Fe-10Cu	80	10	10
Zn-5Fe-15Cu	80	5	15

In this study, iron (Fe) alloy specimens were manufactured by using Fe powders, Zn powders and magnesium (Mg) powders. Iron (Fe) alloy specimens were manufactured by conventional powder metallurgy-mechanical alloying method. Wide range of metal alloy compositions can be fabricated by using mechanical alloying. There is no any phase diagram (solid solubility) restrictions in the mechanical alloying (ball milling). Table given below shows the amounts of alloying elements in the Fe alloys.

- Zinc (Zn) was included in order to increase the biodegradation rate of the Fe. In general biodegradation rate of the pure Fe is very low as compared with bone healing time.
- Magnesium (Mg) was also was included in order to increase the biodegradation rate of the Fe. In general biodegradation rate of the pure Fe is very low as compared with bone healing time.

Table 3.2: Amounts of alloying elements in the Fe alloys

Alloy	Fe	Zn	Mg
Fe-5Zn	95	5	
Fe-10Zn	90	10	
Fe-15Zn	55	15	
Fe-5Mg	95		5
Fe-10Mg	90		10
Fe-15Mg	85		15
Fe-15Zn-5Mg	80	15	5
Fe-10Zn-10Mg	80	10	10
Fe-5Zn-15Mg	80	5	15

In this study, magnesium (Mg) alloy specimens were manufactured by using magnesium (Mg) powders, Zn powders and iron (Fe) powders. Magnesium (Mg) alloy specimens were manufactured by conventional powder metallurgy-mechanical alloying method. Wide range of metal alloy compositions can be fabricated by using mechanical alloying. There is no any phase diagram (solid solubility) restrictions in the mechanical alloying (ball milling). Table given below shows the amounts of alloying elements in the Mg alloys.

- Zinc (Zn) was included in order to decrease the biodegradation rate of the Mg. In general biodegradation rate of the pure Mg is very fast as compared with bone healing time.
- Iron (Fe) was also was included in order to decrease the biodegradation rate of the Mg. In general biodegradation rate of the pure Mg is very low as compared with bone healing time.

Table 3.3: Amounts of alloying elements in the non-porous Mg based specimens

Alloy	Mg	Zn	Fe
Mg-5Zn	95	5	
Mg-10Zn	90	10	
Mg-15Zn	55	15	
Mg-5Fe	95		5
Mg-10Fe	90		10
Mg-15Fe	85		15
Mg-15Zn-5Fe	80	15	5
Mg-10Zn-10Fe	80	10	10
Mg-5Zn-15Fe	80	5	15

Characterization

Microstructure and Mechanical Properties

Microstructure (powder morphology, powder size, sintered microstructure, sinterability and microstructural phases) of the Fe, Mg, and Zn alloy specimens was studied by optical microscope and SEM.

Densities (% porosity) of the Fe, Mg, and Zn alloy specimens were determined by using gravimetric (geometrical) method.

Mechanical properties of the Fe, Mg, and Zn alloy specimens were determined by destructive compression tests (Devotrans, Turkey) and nondestructive ultrasonic tests. Compression-tension device was employed to study the mechanical properties (Devotrans, Turkey).

Elastic modulus of the Fe, Mg, and Zn alloy specimens was also determined by non-destructive ultrasonic testing (USM Go, General Electric). Measurements were carried out by pulse-echo mode transducer having 4 MHz probe.

Biodegradation Properties

In order to study the weight loss, the Zn alloy, Fe alloy, and Mg alloy specimens were dipped inside the simulated body fluid (SBF) solution. Duration inside the SBF was up to four weeks. Metal ion release (Zn, Mg, Fe, and other alloying elements) was measured by using ICP-MS (Thermo Scientific). Gravimetric method was employed in order to measure the weight change of the Zn alloy, Mg alloy, and Fe alloy specimens. pH of the SBF solution was adjusted to 6.50-6.70.

Amounts of the chemical reagents were given below in g/L:

- *NaCl: 8.10 g/L*
- *$MgCl_2$: 0.16 g/L*
- *KCl: 0.38 g/L*
- *$CaCl_2$: 0.12 g/L*
- *Na_2HPO_4: 0.05 g/L*
- *NaH_2PO_4: 0.50 g/L*
- *$NaHCO_3$: 0.37 g/L*
- *Na_2SO_4: 0.04 g/L*
- *Glucose: 1.10 g/L*

Electrochemical Corrosion Tests

Electrochemical corrosion tests were conducted in SBF (simulated (artificial) body fluid) using a potentiostat (Interface 1000, Gamry). High density graphite was counter electrode (cathode), saturated calomel electrode (SCE) was reference electrode and the Zn alloy, Mg alloy, Fe alloy specimens were working electrode (anode). Evaluation of the corrosion results was carried out by a computer software (Gamry)

4. RESULTS

Microsructure

In this study, biodegradable Fe, Zn, and Mg alloy specimens for temporary hard tissue implant applications were fabricated by the pressing-sintering method by using Fe, Zn, and Mg powders. Figure given below illustrates the SEM images of the fine and irregular shaped zinc (Zn) powder, b) iron (Fe) powder, and c) magnesium (Mg) powders.

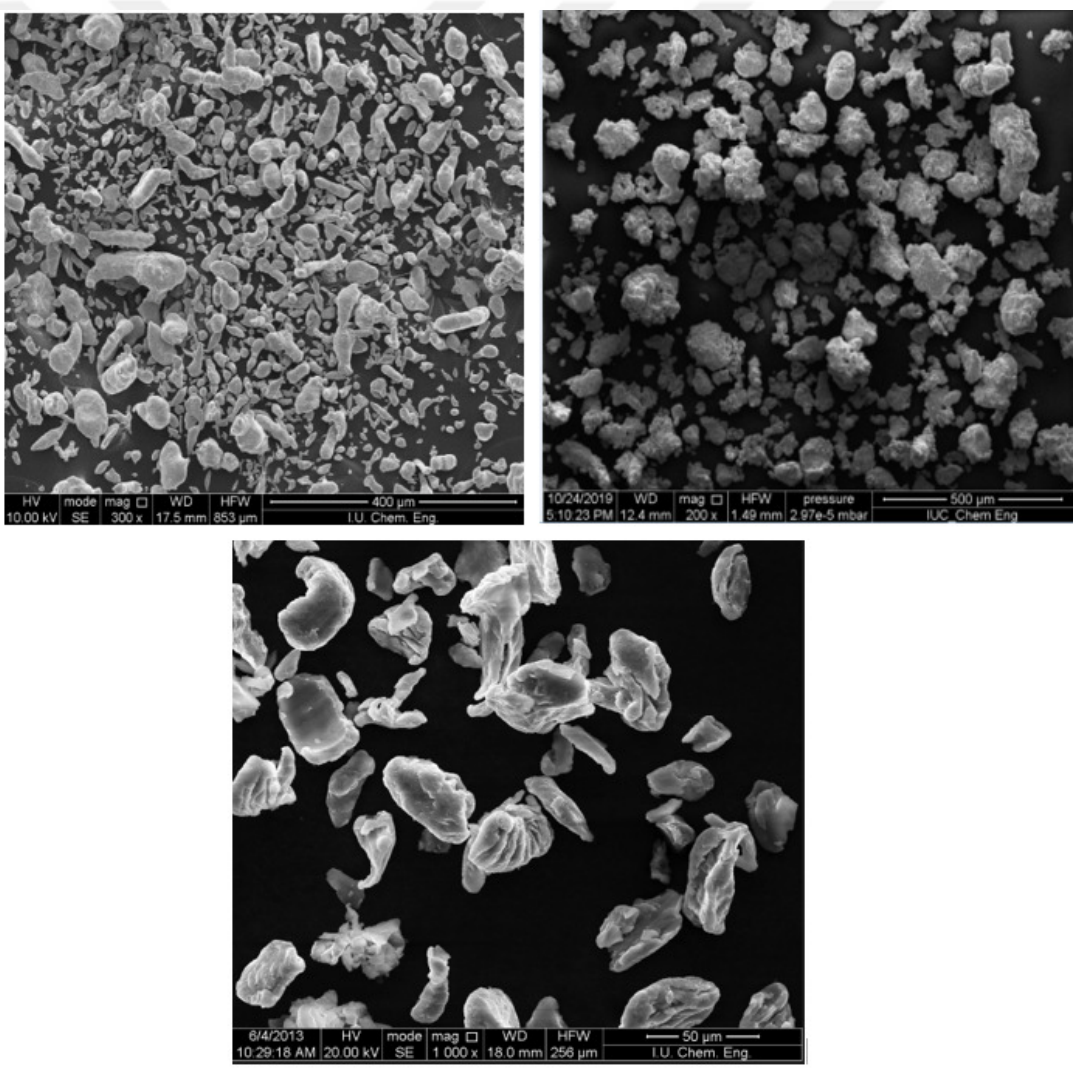

Figure 4.1: SEM picture of a) Zn powder, b) Fe powder, and c) Mg powder

Figure given below shows the optical microscope picture of the sintered zinc (Zn) alloy specimen. As seen from the optical microscope picture, sintering was suitable (sintering temperature and time). There is a suitable bonding between the powders. As seen from the optical microscope picture, there is an uniform microstructure.

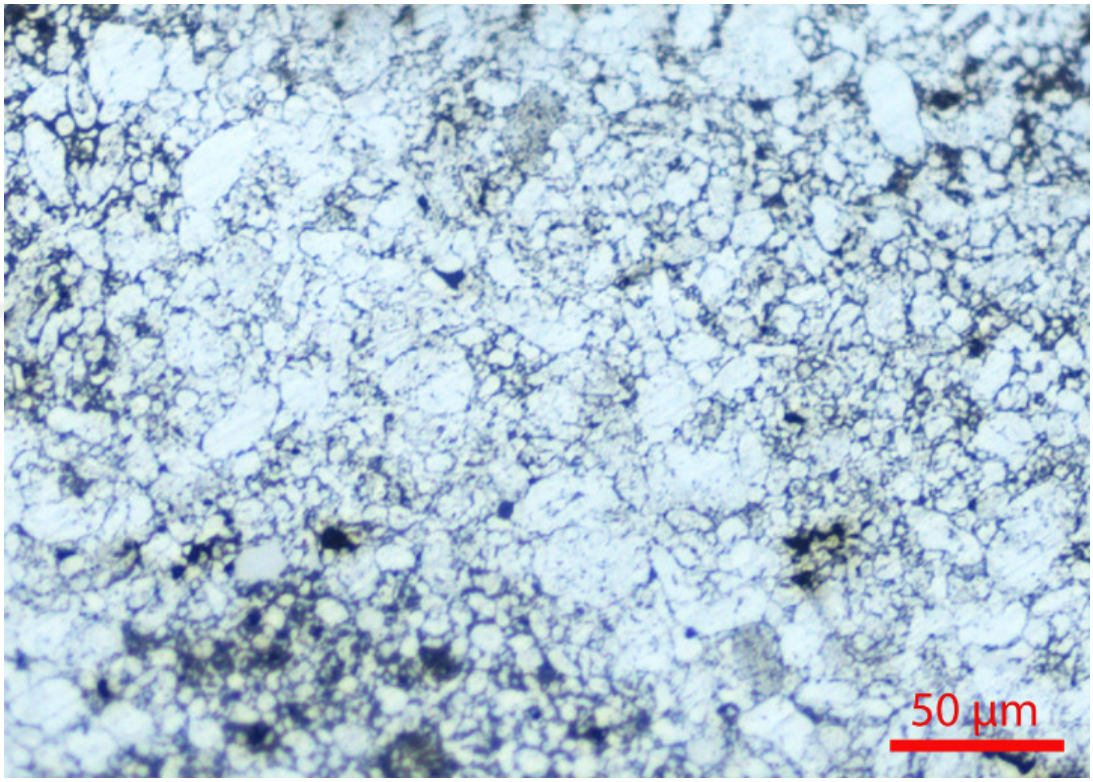

Figure 4.2: Optical microscope picture of sintered Zn-Fe alloy

Figure given below shows the optical microscope picture of the sintered magnesium (Mg) alloy specimen. As seen from the optical microscope picture, sintering was suitable (sintering temperature and time). There is a suitable bonding between the powders. As seen from the optical microscope picture, there is an uniform microstructure

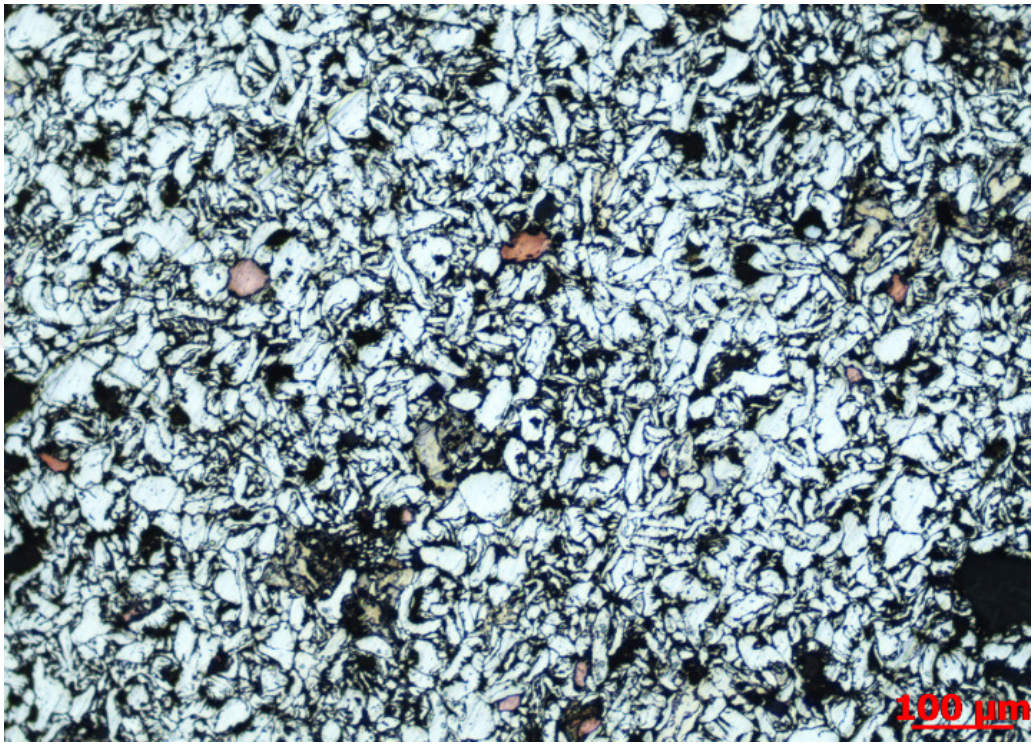

Figure 4.3: Optical microscope picture of sintered Mg-Fe alloy specimen

Figure given below shows the optical microscope picture of the sintered iron (Fe) alloy specimen. As seen from the optical microscope picture, sintering was suitable (sintering temperature and time). There is a suitable bonding between the powders. As seen from the optical microscope picture, there is an uniform microstructure. The microstructure mainly consists of austenite phase and ferrite phase. Also, there are some intermetallics at the grain boundaries.

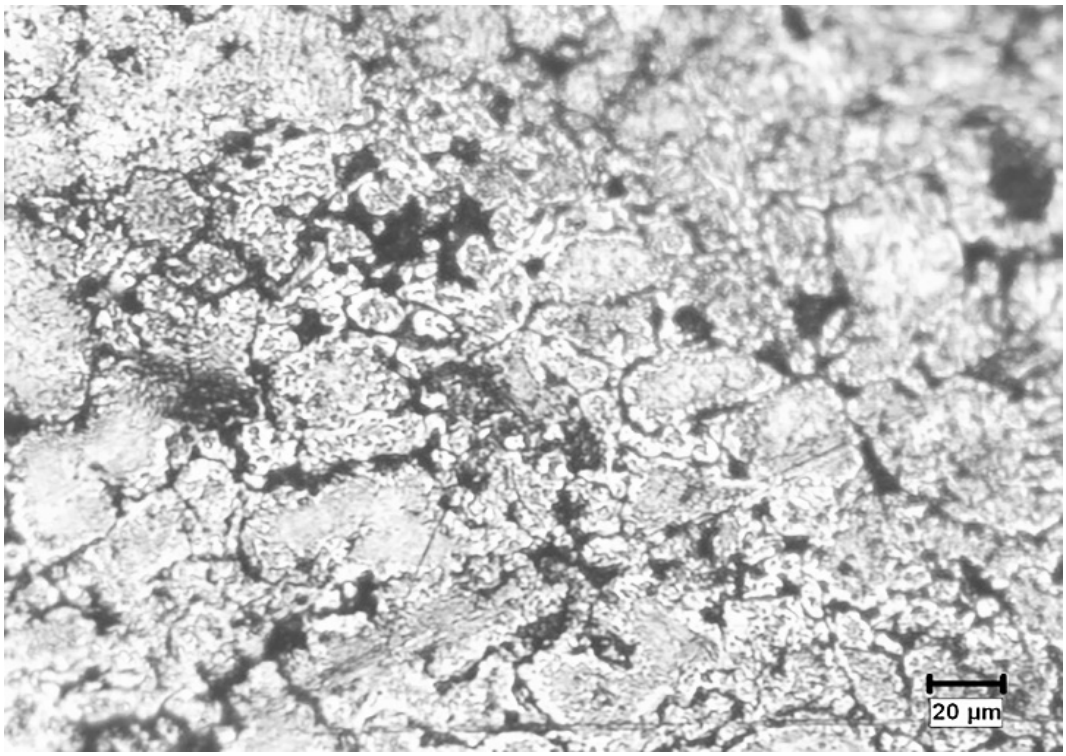

Figure 4.4: Optical microscope picture of sintered Fe-Zn alloy specimen

Figure given below shows the photographs of the sintered iron (Fe) alloy specimens. There is no any shrinkage or any distortion in the shape of the Fe alloy specimens after the sintering.

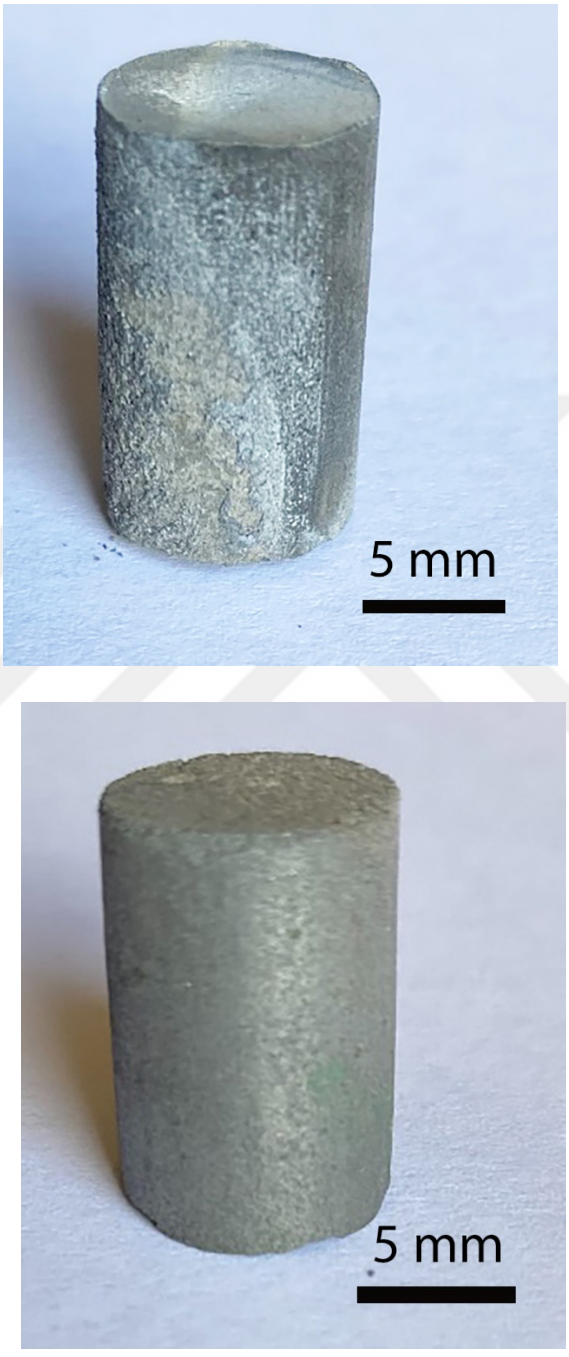

Figure 4.5: Photographs of sintered a) Fe-Mg, and c) Fe-Zn alloy specimens

Figure given below shows the photographs of the sintered magnesium (Mg) alloy specimens. There is no any shrinkage or distortion in the shape of the Mg alloy specimen after sintering.

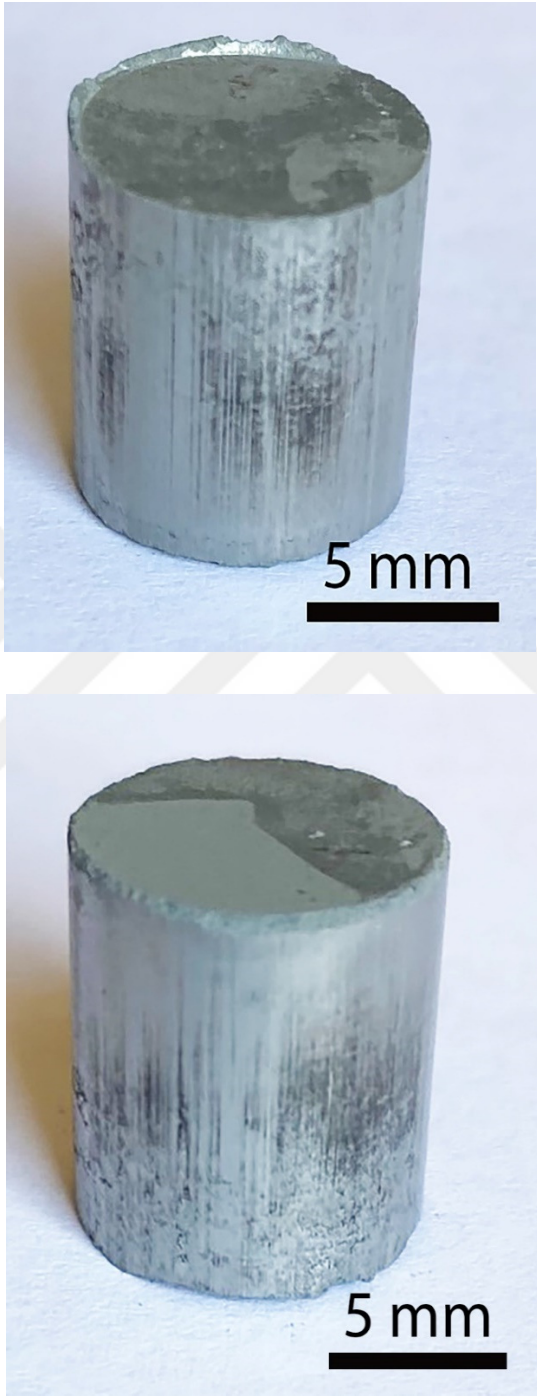

Figure 4.6: Photographs of sintered a) Mg-Fe, and c) Mg-Zn alloy specimens

Figure given below shows the photographs of the sintered zinc (Zn) alloy specimens. There is no any shrinkage or distortion in the shape of the Zn alloy specimen after sintering.

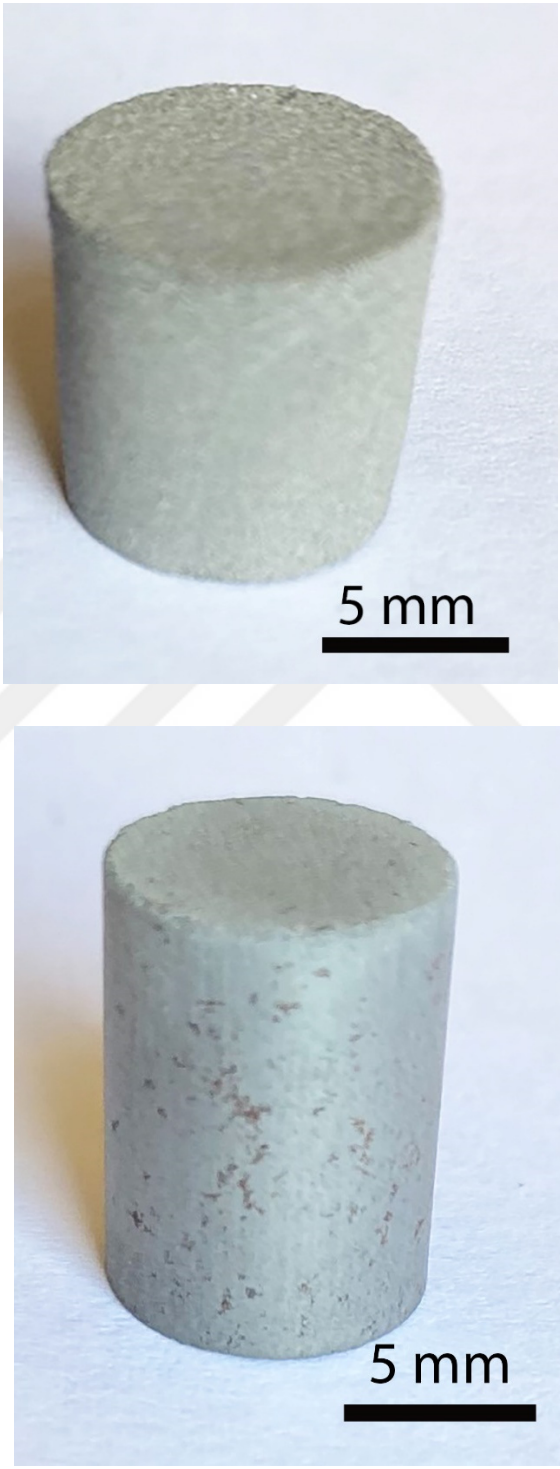

Figure 4.7: Photographs of sintered a) Zn-Fe, and c) Zn-Mg alloy specimens

Mechanical Properties

Table given below illustrates the green density and sintered density values of the Zn alloy specimens. As seen from the table given below, maximum density was obtained in the Zn-5Fe-15Cu alloy specimen, while minimum density was obtained in the Zn-5Fe alloy. Fe and Cu additions were increased the density of the Zn alloy specimens.

Table 4.1: Green and sintered density values of Zn specimens

Alloy	Green Density (g/cm^3)	Sintered Density (g/cm^3)
Zn-5Fe	5.09	5.15
Zn-10Fe	5.15	5.20
Zn-15Fe	5.30	5.40
Zn-5Cu	5.11	5.17
Zn-10Cu	5.22	5.26
Zn-15Cu	5.37	5.46
Zn-15Fe-5Cu	5.41	5.48
Zn-10Fe-10Cu	5.39	5.45
Zn-5Fe-15Cu	5.44	5.50

Table given below illustrates the green density and sintered density values of the Fe alloy specimens. As seen from the table given below, maximum density was obtained in the Fe-5Zn alloy specimen, while minimum density was obtained in the Fe-15Mg alloy. Zn and Mg additions were decreased the density of the Fe alloy specimens.

Table 4.2 Green density and sintered density values of the Fe specimens

Alloy	Green density (g/cm^3)	Sintered density (g/cm^3)
Fe-5Zn	5.15	5.20
Fe-10Zn	5.10	5.12
Fe-15Zn	5.09	5.12
Fe-5Mg	4.91	5.00
Fe-10Mg	4.75	4.81
Fe-15Mg	4.67	4.72
Fe-15Zn-5Mg	5.00	5.02
Fe-10Zn-10Mg	4.82	4.85
Fe-5Zn-15Mg	4.74	4.80

Table given below illustrates the green density and sintered density values of the Mg alloy specimens. As seen from the table, maximum density was obtained in the Mg-5Zn-15Fe alloy specimen, while minimum density was obtained in the Mg-5Zn alloy. Fe and Zn additions were increased the density of the Mg alloy specimens, as expected.

Table 4.3: Green and sintered density values of Mg specimens

Alloy	Green density (g/cm^3)	Sintered density (g/cm^3)
Mg-5Zn	1.60	1.62
Mg-10Zn	1.64	1.66
Mg-15Zn	1.67	1.70
Mg-5Fe	1.66	1.69
Mg-10Fe	1.70	1.73
Mg-15Fe	1.77	1.80
Mg-15Zn-5Fe	1.79	1.81
Mg-10Zn-10Fe	1.77	1.79
Mg-5Zn-15Fe	1.80	1.83

Table given below shows the ultrasonic (nondetsructive) and compression (destructive) elastic modulus values of the sintered zinc (Zn) alloy specimens. Difference between compression test values and ultrasonic test values was in the range of 5-10 %. As seen from the table, maximum elastic modulus was obtained in the Zn-10Fe-10Cu alloy specimen, while minimum elastic modulus was obtained in the Zn-5Fe alloy. Fe and Cu additions were increased the elastic modulus of the specimens.

Table 4.4: Elastic modulus values of the Zn alloy specimens

Alloy	**Elastic modulus (GPa)** *Compression*	**Elastic modulus (GPa)** *Ultrasonic*
Zn-5Fe	81	83
Zn-10Fe	83	85
Zn-15Fe	85	88
Zn-5Cu	83	82
Zn-10Cu	84	85
Zn-15Cu	84	86
Zn-15Fe-5Cu	86	87
Zn-10Fe-10Cu	87	88
Zn-5Fe-15Cu	85	84

Table given below shows the ultrasonic (nondetsructive) and compression (destructive) elastic modulus values of the sintered iron (Fe) alloy specimens. Difference between compression test values and ultrasonic test values was in the range of 5-10 %. As seen from the table, maximum elastic modulus was obtained in the Fe-5Zn alloy specimen, while minimum elastic modulus was obtained in the Fe-15Mg alloy. Zn and Mg additions were decreased the elastic modulus of the specimens, as expected.

Table 4.5: Elastic modulus values of the Fe alloy specimens

Alloy	**Elastic modulus (GPa)** *Compression*	**Elastic modulus (GPa)** *Ultrasonic*
Fe-5Zn	160	162
Fe-10Zn	157	159
Fe-15Zn	155	156
Fe-5Mg	153	150
Fe-10Mg	150	151
Fe-15Mg	148	147
Fe-15Zn-5Mg	156	156
Fe-10Zn-10Mg	155	157
Fe-5Zn-15Mg	151	150

Table given below shows the ultrasonic (nondetsructive) and compression (destructive) elastic modulus values of the sintered magnesium (Mg) alloy specimens. Difference between compression test values and ultrasonic test values was in the range of 5-10 %. As seen from the table, maximum elastic modulus was obtained in the Mg-15Fe alloy specimen, while minimum elastic modulus was obtained in the Mg-10Zn alloy. Zn and Fe additions were increased the elastic modulus of the specimens, as expected.

Table 4.6: Elastic modulus values of the Mg alloy specimens

Alloy	**Elastic modulus (GPa)** *Compression*	**Elastic modulus (GPa)** *Ultrasonic*
Mg-5Zn	30	32
Mg-10Zn	31	30
Mg-15Zn	35	36
Mg-5Fe	33	31
Mg-10Fe	34	33
Mg-15Fe	40	40
Mg-15Zn-5Fe	39	41
Mg-10Zn-10Fe	40	42
Mg-5Zn-15Fe	43	44

Table given below shows the change of the elastic modulus values of the zinc (Zn) alloy specimens with immersion time in the simulated body fluid (SBF) solution. As seen from the table, decrease of the elastic modulus of the Zn alloy specimens was in the range of 12-16 % during 14 days of immersion period in SBF.

Table 4.7: Elastic modulus values of the Zn specimens with immersion time

Alloy	1 day	3 day	7 day	14 day
Zn-5Fe	81	80	75	70
Zn-10Fe	83	77	75	72
Zn-15Fe	85	82	80	75
Zn-5Cu	83	80	70	73
Zn-10Cu	84	83	81	79
Zn-15Cu	84	84	81	80
Zn-15Fe-5Cu	86	84	82	81
Zn-10Fe-10Cu	87	86	83	82
Zn-5Fe-15Cu	85	82	80	79

Table given below shows the change of the elastic modulus values of the iron (Fe) alloy specimens with immersion time in the simulated body fluid (SBF) solution. As seen from the table, decrease of the elastic modulus of the Fe alloy specimens was in the range of 6-15 % during 14 days of immersion period in SBF.

Table 4.8: Elastic modulus values of the Fe specimens with immersion time

Alloy	1 day	3 day	7 day	14 day
Fe-5Zn	155	153	151	147
Fe-10Zn	157	154	152	150
Fe-15Zn	160	159	156	155
Fe-5Mg	153	153	150	148
Fe-10Mg	150	149	147	145
Fe-15Mg	148	148	146	142
Fe-15Zn-5Mg	156	154	153	150
Fe-10Zn-10Mg	155	151	150	148
Fe-5Zn-15Mg	151	151	147	146

Table given below shows the change of the elastic modulus values of the magnesium (Mg) alloy specimens with immersion time in the simulated body fluid (SBF) solution. As seen from the table, decrease of the elastic modulus of the Mg alloy specimens was in the range of 10-25 % during 14 days of immersion period in SBF.

Table 4.9: Elastic modulus values of the Mg specimens with immersion time

Alloy	1 day	3 day	7 day	14 day
Mg-5Zn	30	27	24	21
Mg-10Zn	31	29	26	20
Mg-15Zn	35	31	26	25
Mg-5Fe	33	30	25	24
Mg-10Fe	34	31	27	25
Mg-15Fe	40	37	34	31
Mg-15Zn-5Fe	39	37	35	30
Mg-10Zn-10Fe	40	38	36	31
Mg-5Zn-15Fe	43	41	37	32

Biodegradation Properties

Biodegradation behaviour of the metal alloy specimens was studied by weight change and metal ion release measurements in simulated body fluid solutions. Metal ion (Zn^{2+}, Cu^{2+}, $Mg^{2+}$and Fe^{3+}/Fe^{2+}) release values from the specimens were increased with increasing immersion time in the simulated body fluid (SBF) solution, as expected.

Table 4.10: Amounts of release of alloying elements from Zn alloys in the SBF

Alloy	Zn (ppm)	Fe (ppm)	Cu (ppm)
Zn-5Fe	206	12	
Zn-10Fe	201	22	
Zn-15Fe	200	25	
Zn-5Cu	195		4
Zn-10Cu	193		7
Zn-15Cu	195		10
Zn-15Fe-5Cu	192	22	3
Zn-10Fe-10Cu	190	25	6
Zn-5Fe-15Cu	191	15	12

Table 4.11: Weight change of the Zn alloys in the SBF

Alloy	Weight change (%)
Zn-5Fe	25
Zn-10Fe	23
Zn-15Fe	20
Zn-5Cu	22
Zn-10Cu	20
Zn-15Cu	16
Zn-15Fe-5Cu	18
Zn-10Fe-10Cu	15
Zn-5Fe-15Cu	14

Figure given below illustrates the metal ion (Zn^{2+}, Mg^{2+}, and Fe^{3+}/Fe^{2+}) release values from the Fe alloy specimens in simulated body fluid (SBF) solutions. .

Table 4.12: Amounts of release of alloying elements from Fe alloys in the SBF

Alloy	Fe (ppm)	Zn (ppm)	Mg (ppm)
Fe-5Zn	65	5	
Fe-10Zn	66	7	
Fe-15Zn	70	8	
Fe-5Mg	67		12
Fe-10Mg	70		16
Fe-15Mg	72		22
Fe-15Zn-5Mg	72	9	13
Fe-10Zn-10Mg	73	7	19
Fe-5Zn-15Mg	71	7	26

Table 4.13: Weight change of the Fe alloys in the SBF

Alloy	Weight change (%)
Fe-5Zn	2
Fe-10Zn	4
Fe-15Zn	5
Fe-5Mg	5
Fe-10Mg	10
Fe-15Mg	12
Fe-15Zn-5Mg	12
Fe-10Zn-10Mg	13
Fe-5Zn-15Mg	16

Figure given below illustrates the metal ion (Zn^{2+}, Mg^{2+}, and Fe^{3+}/Fe^{2+}) release values from the Mg alloy specimens in simulated body fluid (SBF) solutions.

Table 4.14: Amounts of release of alloying elements from Mg alloys in the SBF

Alloy	Mg (ppm)	Zn (ppm)	Fe (ppm)
Mg-5Zn	320	6	
Mg-10Zn	310	6	
Mg-15Zn	302	8	
Mg-5Fe	311		1
Mg-10Fe	304		2
Mg-15Fe	294		2
Mg-15Zn-5Fe	293	6	1
Mg-10Zn-10Fe	292	5	1
Mg-5Zn-15Fe	293	5	2

Table 4.15: Weight change of the Mg alloys in the SBF

Alloy	Weight change (%)
Mg-5Zn	33
Mg-10Zn	30
Mg-15Zn	28
Mg-5Fe	31
Mg-10Fe	28
Mg-15Fe	25
Mg-15Zn-5Fe	24
Mg-10Zn-10Fe	23
Mg-5Zn-15Fe	20

Electrochemical Corrosion Tests

In addition, the biodegradation behaviour of the alloys was studied by electrochemical corrosion tests in the simulated body fluid solutions. Table given below shows the electrochemical corrosion rate values of the different Zn alloys in the simulated body fluid (SBF) solution.

Table 4.16: Corrosion rates of the Zn alloys in the SBF solution

Alloy	Corrosion Rate (mm/year)
Zn-5Fe	0.23
Zn-10Fe	0.22
Zn-15Fe	0.20
Zn-5Cu	0.21
Zn-10Cu	0.18
Zn-15Cu	0.17
Zn-15Fe-5Cu	0.14
Zn-10Fe-10Cu	0.14
Zn-5Fe-15Cu	0.13

Table given below shows the electrochemical corrosion rate values of the different Fe alloys in the simulated body fluid (SBF) solution.

Table 4.17: Corrosion rate values of the Fe alloys in the SBF solution

Alloy	Corrosion Rate (mm/year)
Fe-5Zn	0.01
Fe-10Zn	0.02
Fe-15Zn	0.05
Fe-5Mg	0.05
Fe-10Mg	0.11
Fe-15Mg	0.12
Fe-15Zn-5Mg	0.11
Fe-10Zn-10Mg	0.12
Fe-5Zn-15Mg	0.14

Table given below shows the electrochemical corrosion rate values of the different Mg alloys in the simulated body fluid (SBF) solution.

Table 4.18: Corrosion rate values of the Mg alloys in the SBF solution

Alloy	Corrosion Rate (mm/year)
Mg-5Zn	2.1
Mg-10Zn	1.8
Mg-15Zn	1.7
Mg-5Fe	2.0
Mg-10Fe	1.6
Mg-15Fe	1.3
Mg-15Zn-5Fe	1.3
Mg-10Zn-10Fe	1.4
Mg-5Zn-15Fe	1.2

5. DISCUSSION

In the present study, biodegradable metal (Fe, Zn, and Mg) alloys for temporary biomedical implant applications were fabricated and investigated. Biodegradable metal alloys (Fe, Zn, and Mg) were fabricated by mechanical alloying-powder metallurgy method. Temporary biomedical implants for hard tissue applications, must show elastic modulus close to bone (to prevent stress-shielding effect), must show optimum biodegradation rate close to bone healing rate, and must have suitable biocompatibility level. Initially, metal powders were processed in ball mill (mechanical alloying), then polymer based binder was included, then the mixture was compacted and green specimens were fabricated, and lastly the green specimens were sintered. Electrochemical corrosion properties of the alloys were investigated in simulated body fluid with potentiostat. In addition, metal ion (Fe, Zn, and Mg) release and weight change properties of the alloys were investigated in simulated body fluid. In general, biomaterial is a systemically and pharmacologically inert material manufactured for implantation within or incorporation with living systems. In general, biomaterials are a group of advanced engineering materials. In the periodic table, although approximately 3/4 of the elements are metal, small number metals can be employed in the biomedical applications due to their low biocompatibility (materials with low toxicity) which is attributed to their electrochemical corrosion. The term “biomaterial can be desribed as nonliving material group employed in a biomedical device, aimed to interact with biological organs/tissues. This definition, also can be changed as material group aimed to interface with biological tissue/organs in order to repair, treat, heal or replace any living organ or tissue. Biomaterials (biocompatible materials) are sysnthetic materials employed in the body mainly for their mechanical properties, but not biological properties. In general, biocompatibility can be defined as the behaviour/property of a material group, which shows a suitable host response in a definite usage [9]. Biomedical implants can be described as a medical device, which is manufactured by biomaterials, used in the living body. The biomedicsl implants are employed in the lining body in order to replace or repair of damaged tissue/organs [1-12].

There was no any shrinkage or distortion in the shape of the Zn alloy, Mg alloy and Fe alloy specimens after sintering process.

Densities of the specimens were determined by geometrical method. Maximum density was obtained in the Zn-5Fe-15Cu alloy specimen, while minimum density was obtained in the Zn-5Fe alloy. Fe and Cu additions were increased the density of the Zn alloy specimens. Maximum density was obtained in the Fe-5Zn alloy specimen, while minimum density was obtained in the Fe-15Mg alloy. Zn and Mg additions were decreased the density of the Fe alloy specimens. Maximum density was obtained in the Mg-5Zn-15Fe alloy specimen, while minimum density was obtained in the Mg-5Zn alloy. Fe and Zn additions were increased the density of the Mg alloy specimens.

Maximum elastic modulus was obtained in the Zn-10Fe-10Cu alloy specimen, while minimum elastic modulus was obtained in the Zn-5Fe alloy. Fe and Cu additions were increased the elastic modulus of the specimens. Maximum elastic modulus was obtained in the Fe-5Zn alloy specimen, while minimum elastic modulus was obtained in the Fe-15Mg alloy. Zn and Mg additions were decreased the elastic modulus of the specimens. Maximum elastic modulus was obtained in the Mg-15Fe alloy specimen, while minimum elastic modulus was obtained in the Mg-10Zn alloy. Zn and Fe additions were increased the elastic modulus of the specimens.

Change of the elastic modulus values of the magnesium (Mg), zinc (Zn), and iron (Fe) alloy specimens with immersion time in the simulated body fluid (SBF) solution was determined. Decrease of the elastic modulus of the Fe alloy specimens was in the range of 6-15 % during 14 days of immersion period in SBF. Decrease of the elastic modulus of the Zn alloy specimens was in the range of 12-16 % during 14 days of immersion period in SBF. Decrease of the elastic modulus of the Mg alloy specimens was in the range of 10-25 % during 14 days of immersion period in SBF.

Figure given below shows the Pourbaix diagram (E-pH diagram) of the zinc (Zn). As shown from the figure, Zn and Zn alloys can show biodegradation at the body conditions, as expected.

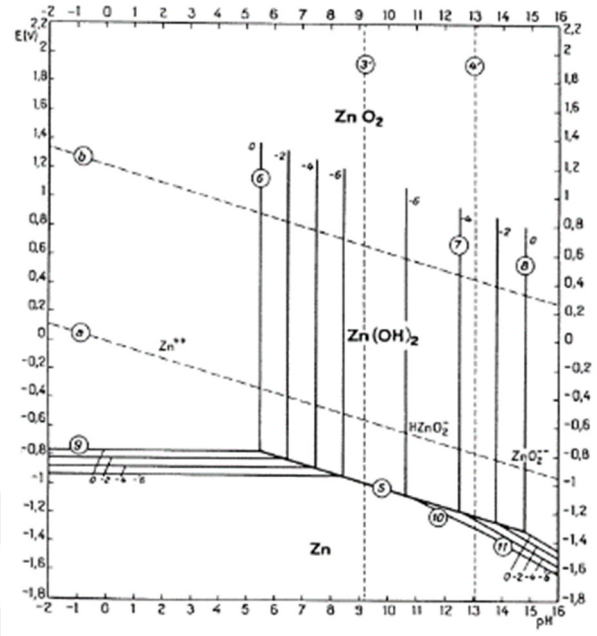

Figure 5.1: Pourbaix diagram of Zn [13]

Figure given below shows the Pourbaix diagram (E-pH diagram) of the iron (Fe). As shown from the figure, Fe and Fe alloys can show biodegradation at the body conditions, as expected.

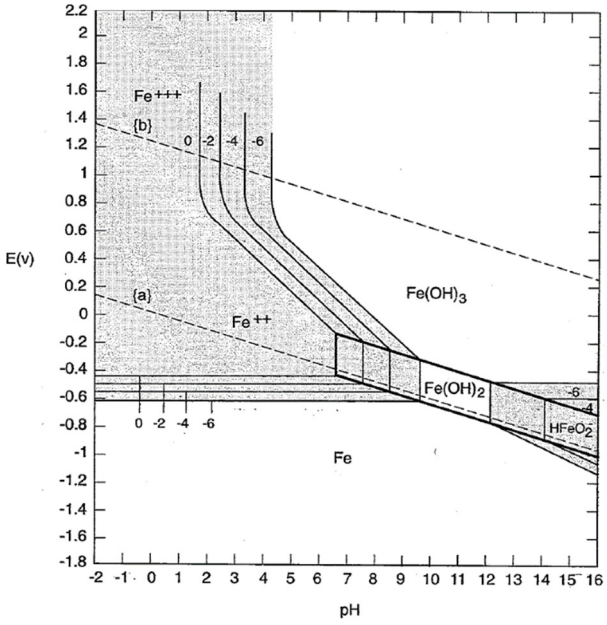

Figure 5.2: Pourbaix diagram of Fe [14]

Magnesium (Mg) is a very active metal and body fluids can easily dissolves the Mg and Mg alloys. Figure given below illustrates the Pourbaix diagram of the magnesium (Mg)[14]. As shown from the figure, Mg alloys can show biodegradation at the body conditions, as expected.

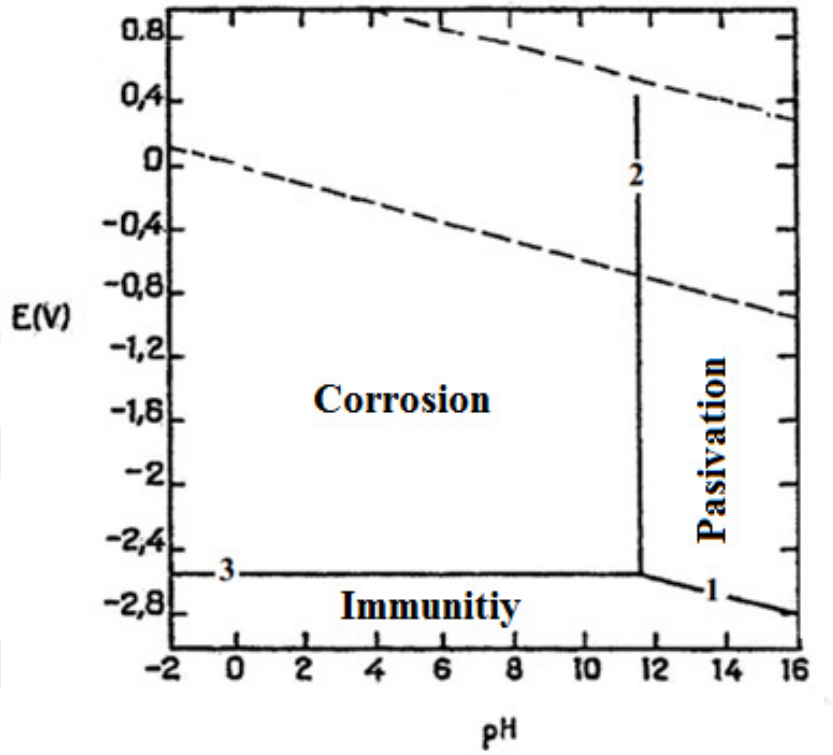

Figure 5.3: Pourbaix diagram of the Mg [14]

6. CONCLUSION AND RECOMMENDATIONS

In the present study, biodegradable metal (Fe, Zn, and Mg) alloys for temporary biomedical implant applications were fabricated and investigated. Biodegradable metal alloys (Fe, Zn, and Mg) were fabricated by mechanical alloying-powder metallurgy method. Temporary biomedical implants for hard tissue applications, must show elastic modulus close to bone (to prevent stress-shielding effect), must show optimum biodegradation rate close to bone healing rate, and must have suitable biocompatibility level. Initially, metal powders were processed in ball mill (mechanical alloying), then polymer based binder was included, then the mixture was compacted and green specimens were fabricated, and lastly the green specimens were sintered. Electrochemical corrosion properties of the alloys were investigated in simulated body fluid with potentiostat. In addition, metal ion (Fe, Zn, and Mg) release and weight change properties of the alloys were investigated in simulated body fluid.

Biomaterial is a systemically and pharmacologically inert material manufactured for implantation within or incorporation with living systems. Biomaterials are a group of advanced engineering materials. In the periodic table, although approximately 3/4 of the elements are metal, small number metals can be employed in the biomedical applications due to their low biocompatibility (materials with low toxicity) which is attributed to their electrochemical corrosion. The term “biomaterial (biocompatible materials)” can be desribed as nonliving material group employed in a biomedical device, aimed to interact with biological organs/tissues. This definition, also can be changed as material group aimed to interface with biological tissue/organs in order to repair, treat, heal or replace any living organ or tissue. In general, the biomaterials (biocompatible materials) are sysnthetic materials employed in the body mainly for their mechanical properties, but not biological properties. In general, biocompatibility can be defined as the behaviour/property of a material group, which shows a suitable host response in a definite usage [9]. Biomedical implants can be described as a medical device, which is manufactured by biomaterials, used in the living body. The biomedicsl implants are employed in the lining body in order to replace or repair of damaged tissue/organs [1-12].

General Conclusions:

- As the biodegradation rate is low or moderate, Zn and Zn alloys should be used as a biodegradable temporaty screw or plate in the bone healing (bone fracture) applications.
- As the biodegradation rate is very high or high, Mg allyoys are more suitable for soft tissue applications or scaffold material in the tissue engineering applications.
- As the biodegradation rate is very low or low, Fe and Fe alloys are more suitable to the orthopaedic implant (shoulder, total knee or total hip) applications.

REFERENCES

[1] Park J.B., Bronzino J.D.. 2007, Biomaterials, Principles and Applications, CRC Press, New York, USA.

[2] Pruitt L, 2011, Mechanics of Biomaterials, Fundamental Principles for Implant Design. Cambridge University Press, Cambridge, UK.

[3] Hendra Hermawan, 2012, Biodegradable Metals, From Concepts to Applications. Springer, London, UK

[4] Yang H, Wang C, Liu C, Chen H, Wu Y, Han J *et al* 2017 *Biomaterials* **145** 92

[5] Ratner, B. 2004, Biomaterials Science, An Introduction to Materials in Medicine, Elsevier.

[6] Vojtech D, Kubasek J, Serak J and Novak P 2011 *Acta Biomater* **7** 3515

[7] Zhao S, Seitz J M, Eifler R, Maier H J, Guillory R J, Earley E J *et al* 2017 *Mater Sci Eng C* **76** 301

[8] Einar Bardal. 2003, Corrosion and Protection, Engineering Materials and Processes, Springer, London, UK.

[9] Hasırcı V. Hasırcı N. 2018, Fundamentals of Biomaterials. Springer, New York, USA.

[10] Agarwal R. Garcia A.J. 2015, Advanced Drug Delivery Reviews, 94, 53-62.

[11] Liu Y. Zheng Y, Chen C.C. Yang J. Pan H. Chen D. Wang L. Zhang J. Zhu D. Wu S. Yeung K.W.K. Zeng R. Han Y. Guan S. 2019, Biodegradable metals. Advanced Functional Materials 29, 1805402.

[12] Ramakrishna S. Huang Z.M. Kumar G.V. Batchelor A.W. Mayer J. 2004, An Introduction to Biocomposites, Vol. I, Imperial College Press.

[13] Zhang X.G. 1996, Corrosion and Electrochemistry of Zinc, Springer Press.

[14] Jones, D.A., 1996. *Principles and Prevention of Corrosion*, Second Edition, Prentice Hall, USA.

[15] Bowen P K, Guillory R J, Shearier E R, Seitz J M, Drelich J, Bocks M, *et al* 2015 *Mater Sci Eng C* **56** 467

[16] Drelich A J, Zhao S, Guillory R J, Drelich J W and Goldman J 2017 *Acta Biomater* **58** 539

[17] Y.F. Zheng, X.N. Gu, F. Witte. 2014, Biodegradable Metals. Materials Science and Engineering R 77, 1-34.

[18] Sadighikia S, Abdolhosseinzadeh S and Asgharzadeh H 2015 *Powder Met.* 58, **1** 61

[19] Azizi A and Haghighi G G 2015 *Int J Adv Manuf Technol.* **77** 2059

[20] Berent K, Pstrus J and Gancarz T 2016 *J Mater Eng Perform* **25** 3375

[21] Kafri A, Ovadia S, Goldman J, Drelich J and Aghion E 2018 *Metals* **8** 153

FIRST PAGE OF THE PLAGIARISM REPORT

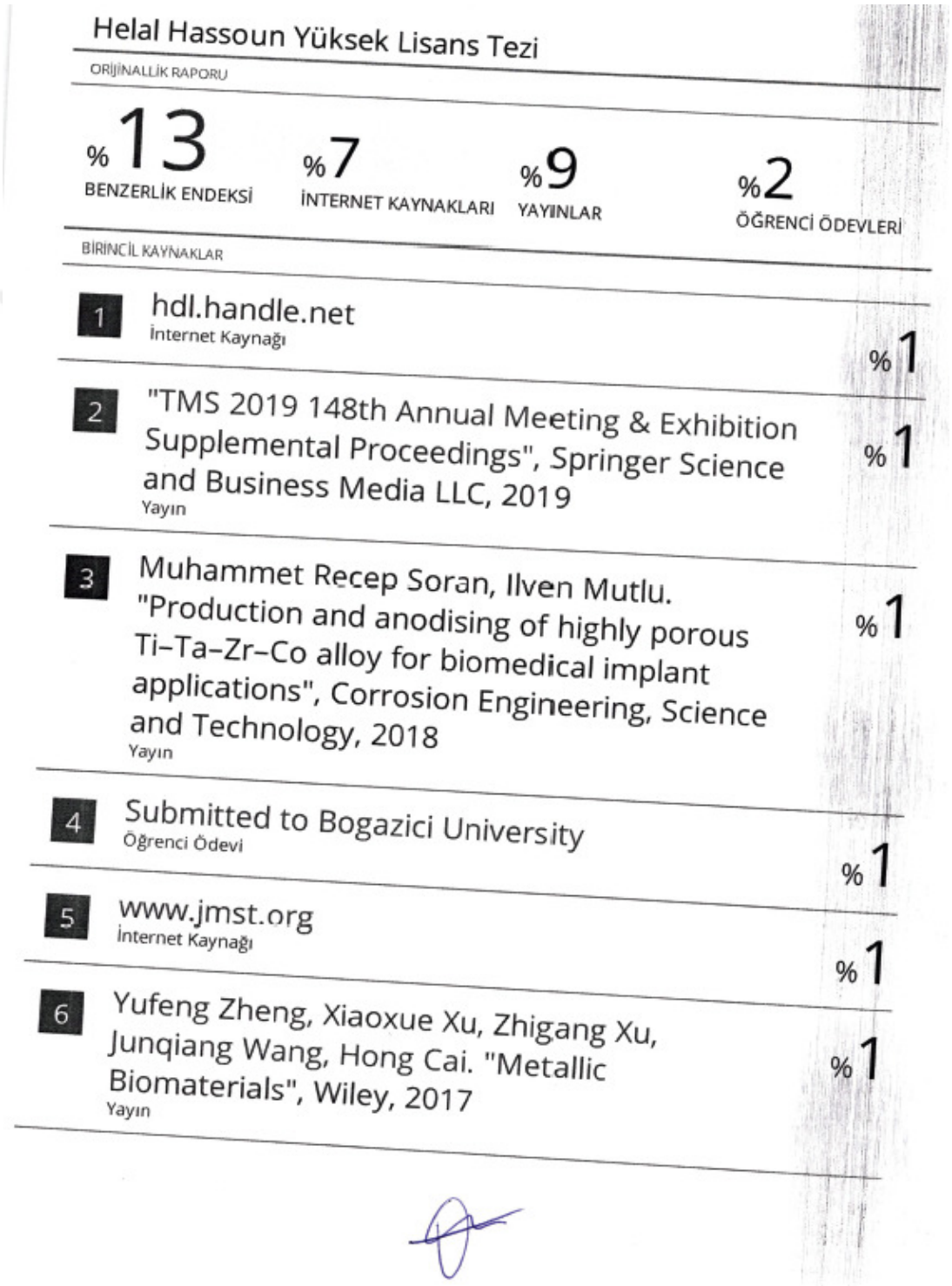

Helal Hassoun Yüksek Lisans Tezi

ORİJİNALLİK RAPORU

%13	%7	%9	%2
BENZERLİK ENDEKSİ	İNTERNET KAYNAKLARI	YAYINLAR	ÖĞRENCİ ÖDEVLERİ

BİRİNCİL KAYNAKLAR

1	hdl.handle.net İnternet Kaynağı	%1
2	"TMS 2019 148th Annual Meeting & Exhibition Supplemental Proceedings", Springer Science and Business Media LLC, 2019 Yayın	%1
3	Muhammet Recep Soran, Ilven Mutlu. "Production and anodising of highly porous Ti–Ta–Zr–Co alloy for biomedical implant applications", Corrosion Engineering, Science and Technology, 2018 Yayın	%1
4	Submitted to Bogazici University Öğrenci Ödevi	%1
5	www.jmst.org İnternet Kaynağı	%1
6	Yufeng Zheng, Xiaoxue Xu, Zhigang Xu, Junqiang Wang, Hong Cai. "Metallic Biomaterials", Wiley, 2017 Yayın	%1

ETHICS COMMITTEE PERMISSION

WARNING: It is mandatory to obtain an Ethics Committee Permission for all research topics related to living subjects.

☐ **Ethics Committe permission is required.**

☒ **Ethics Committe permission is not required.**

Helal HASSOUN

(Signature)

INSTITUTIONAL PERMISSIONS

WARNING: It is mandatory to obtain Institutional Permission for all research topics related to living and dead subjects. In cases involving confidentiality and privacy, the name of the institution should be closed.

☐ **Institutional permission is required.**

☒ **Institutional permission is not required.**

Helal HASSOUN

(Signature)

CURRICULUM VITAE

Personal Information	
Name Surname	----
Birth Date	-----
Nationality	❒ T.C. ❒ Other:
E-Mail	
Website	

Education	
Undergraduate	
University	
Faculty	
Department	
Graduation Year	
Master of Science	
University	
Faculty	
Department	
Graduation Year	

Publications